Adv Comput Math manuscript No.
(will be inserted by the editor)

Virtual element methods for the three-field formulation of time-dependent linear poroelasticity

Raimund Bürger · Sarvesh Kumar · David Mora · Ricardo Ruiz-Baier · Nitesh Verma

October 23, 2020

Abstract A virtual element discretisation for the numerical approximation of the three-field formulation of linear poroelasticity introduced in [R. Oyarzúa and R. Ruiz-Baier, Locking-free finite element methods for poroelasticity, *SIAM J. Numer. Anal.* **54** (2016) 2951–2973] is proposed. The treatment is extended to include also the transient case. Appropriate poroelasticity projector operators are introduced and they assist in deriving energy bounds for the time-dependent discrete problem. Under standard assumptions on the computational domain, optimal a priori error estimates are established. These estimates are valid independently of the values assumed by the dilation modulus and the specific storage coefficient, implying that the formulation is locking-free. Furthermore, the accuracy of the method is verified numerically through a set of computational tests.

Keywords Biot equations · virtual element method · time-dependent problems · a priori error analysis

Mathematics Subject Classification (2010) 65M60 · 74F10 · 35K57 · 74L15.

1 Introduction

The equations of linear poroelasticity describe the interaction between interstitial fluid flowing through deformable porous media. This problem, often referred to as Biot's consolidation problem, has a wide range of applications in diverse areas including biomechanics, groundwater management, oil extraction, earthquake engineering, and material sciences [7, 37, 38].

R. Bürger
Centro de Investigación en Ingeniería Matemática (CI^{2}MA) and Departamento de Ingeniería Matemática, Universidad de Concepción, Casilla 160-C, Concepción, Chile.
E-mail: rburger@ing-mat.udec.cl

S. Kumar, N. Verma
Department of Mathematics, Indian Institute of Space Science and Technology, Trivandrum 695 547, India.
E-mail: sarvesh@iist.ac.in, niteshverma.16@res.iist.ac.in

D. Mora
GIMNAP, Departamento de Matemática, Universidad del Bío-Bío, Concepción, Chile; and CI^{2}MA, Universidad de Concepción, Chile.
E-mail: dmora@ubiobio.cl

R. Ruiz-Baier
School of Mathematical Sciences, Monash University, 9 Rainforest Walk, Clayton VIC 3800, Australia; and Laboratory of Mathematical Modelling, Institute of Personalised Medicine, Sechenov University, Moscow, Russian Federation.
E-mail: ricardo.ruizbaier@monash.edu

A variety of numerical methods has been used to generate approximate solutions to Biot's consolidation problem. Modern examples include high-order finite differences [25], conforming finite elements [43], mixed finite element methods [29], nodal and local discontinuous Galerkin methods [30, 47], finite volume schemes [8], and combined/hybrid discretisations [23, 24, 33]; we further point out [14] where the authors present a polygonal discretisation based on hybrid high-order methods. These schemes are constructed using different formulations of the governing equations including primal and several types of mixed forms.

In this paper we propose a virtual element method (VEM) using a three-field formulation of the time-dependent poromechanics equations. We base the development following the formulation proposed in [34,35] and [45] for the stationary Biot system and extend the discrete analysis to include the quasi-steady case.

Although the VEM is relatively recent, it has been already applied to a large number of problems; for instance, Stokes, Brinkman, Cahn-Hilliard, plate bending, Helmholtz, and parabolic problems have studied using VEM in [3, 5, 6, 11, 13, 18, 20, 22, 46, 50, 51], whereas a coupled VEM-finite volume formulation for the Biot equations has been proposed in [23]. Recently, VEM has been also developed in [49] with another three-field formulation (seen in [53]) for the Biot's equation. Advantages of VEM include the relaxation of computing basis functions (of particular usefulness when dealing with high-order approximations), and the flexibility of computing solutions on general-shaped meshes (for instance, including non-convex elements). In addition, one works locally on polygonal elements, without the need of passing through a reference element, see, e.g., [1, 9, 10, 41]. In principle, this further simplifies the implementation of the building blocks of the numerical method. We observe that in complex simulations like phase change, fluid-structure interaction, and many others, the geometrical complexity of the domain is a relevant issue when PDEs have to be solved on a good-quality mesh; hence, it can be convenient to use more general polygonal/polyhedral meshes.

Here we consider a pair of virtual elements for displacement and total pressure which is stable. This pair, introduced in [5], can be regarded as a generalisation of the Bernardi-Raugel finite elements (piecewise linear elements enriched with bubbles normal to the faces for the displacement components, and piecewise constant approximations for total pressure, see, e.g., [27]). On the other hand, no compatibility between the spaces for total pressure and fluid pressure is needed. Therefore for the fluid pressure we employ the enhanced virtual element space from [3, 10, 51], which allows us to construct a suitable projector onto piecewise linear functions. All this is restricted, for sake of simplicity, to the lowest-order 2D case, but one could extend the analysis to higher polynomial degrees and the 3D case, for instance considering the discrete inf-sup stable pair from [11] for the Stokes problem. The main difficulties in our analysis lie in the definition of an adequate projection operator that allows to treat the time-dependent problem. To handle this issue we have combined Stokes-like and elliptic operators that constitute the new map, here named poroelastic projector. We derive stability for semi-discrete and fully-discrete approximations and establish the optimal convergence of the virtual element scheme in the natural norms. These bounds turn to be robust with respect to the dilation modulus of the deformable porous structure (which tends to infinity as the Poisson ratio approaches 0.5), and of the specific storage coefficient (reaching very small values in some regimes), and therefore the method is considered locking-free. A further advantage of the proposed virtual discretisation is that it combines primal and mixed virtual element spaces. In addition, this work can be seen as a stepping stone in the study of more complex coupled problems including interface poroelastic phenomena and multiphysics (see, for instance, [4, 26, 52]).

We have arranged the contents of the paper as follows. Section 2 is devoted to the definition of the linear poroelasticity problem, and it also contains the precise definition of the continuous weak formulation using three fields, and presents a few preliminary results needed in the semi-discrete analysis as well. In Section 3 we introduce the virtual element approximation in semi-discrete form. We specify the virtual element spaces, we identify the degrees of freedom, and derive appropriate estimates for the discrete bilinear forms. The a priori error analysis has been derived in Section 4, with the help of the newly introduced poroelastic projection operator. The implementation of the problem on different families of polygonal meshes is then discussed in Section 5, where we confirm the theoretical rates of convergence and produce some applicative tests to gain insight on the behaviour of the model problem. A summary and concluding remarks are collected in Section 6.

2 Time-dependent linear poroelasticity using total pressure

2.1 Strong form of the governing equations

A deformable porous medium is assumed to occupy the domain Ω, where Ω is an open and bounded set in $\mathbb{R}^2$ (simply for sake of notational convenience) with a Lipschitz continuous boundary $\partial\Omega$. The medium is composed by a mixture of incompressible grains forming a linearly elastic skeleton, as well as interstitial fluid. The mathematical description of this interaction between deformation and flow can be placed in the context of the classical Biot problem, written as follows (see for instance, the exposition in [48]). In the absence of gravitational forces, and for a given body load $\boldsymbol{b}(t) : \Omega \to \mathbb{R}^2$ and a volumetric source or sink $\ell(t) : \Omega \to \mathbb{R}$, one seeks, for each time $t \in (0, t_{\text{final}}]$, the vector of displacements of the porous skeleton, $\boldsymbol{u}(t) : \Omega \to \mathbb{R}^2$, and the pore pressure of the fluid, $p(t) : \Omega \to \mathbb{R}$, satisfying the mass conservation of the fluid content and momentum balance equations

$$\begin{aligned} \partial_t(c_0 p + \alpha \operatorname{div} \boldsymbol{u}) - \frac{1}{\eta} \operatorname{div}\big(\kappa(\boldsymbol{x})\nabla p\big) &= \ell, \\ -\,\mathbf{div}\big(\lambda(\operatorname{div} \boldsymbol{u})\boldsymbol{I} + 2\mu\boldsymbol{\varepsilon}(\boldsymbol{u}) - \alpha p \boldsymbol{I}\big) &= \rho \boldsymbol{b} \quad \text{in } \Omega \times (0, t_{\text{final}}], \end{aligned}$$

where $\kappa(\boldsymbol{x})$ is the hydraulic conductivity of the porous medium (the mobility matrix, possibly anisotropic), ρ is the density of the solid material, η is the constant viscosity of the interstitial fluid, c_0 is the constrained specific storage coefficient (typically small and representing the amount of fluid that can be injected during an increase of pressure maintaining a constant bulk volume), α is the Biot-Willis consolidation parameter (typically close to one), and μ and λ are the shear and dilation moduli associated with the constitutive law of the solid structure. The total stress

$$\boldsymbol{\sigma} = \lambda(\operatorname{div} \boldsymbol{u})\boldsymbol{I} + 2\mu\boldsymbol{\varepsilon}(\boldsymbol{u}) - \alpha p \boldsymbol{I}$$

includes a contribution from the effective mechanical stress of a Hookean elastic material, $\boldsymbol{\sigma}_{\text{eff}} = \lambda(\operatorname{div} \boldsymbol{u})\boldsymbol{I} + 2\mu\boldsymbol{\varepsilon}(\boldsymbol{u})$, and the non-viscous fluid stress represented only by the pressure scaled with α. As in [35,45], we consider here the volumetric part of the total stress ψ, hereafter called *total pressure*, as one of the primary variables. This property allows us to rewrite the time-dependent problem as

$$\begin{aligned} -\,\mathbf{div}\big(2\mu\boldsymbol{\varepsilon}(\boldsymbol{u}) - \psi\boldsymbol{I}\big) &= \rho\boldsymbol{b}, \\ \left(c_0 + \frac{\alpha^2}{\lambda}\right)\partial_t p - \frac{\alpha}{\lambda}\partial_t\psi - \frac{1}{\eta}\operatorname{div}(\kappa\nabla p) &= \ell, \\ \psi - \alpha p + \lambda \operatorname{div} \boldsymbol{u} &= 0 \quad \text{in } \Omega \times (0, t_{\text{final}}], \end{aligned} \tag{2.1}$$

which we endow with appropriate initial data

$$p(0) = p^0, \quad \boldsymbol{u}(0) = \boldsymbol{u}^0 \quad \text{in } \Omega \times \{0\},$$

(which, in turn, can be used to set the initial condition for the total pressure $\psi(0)$), and mixed-type boundary conditions in the following manner

$$\boldsymbol{u} = \boldsymbol{0} \quad \text{and} \quad \frac{\kappa}{\eta}\nabla p \cdot \boldsymbol{n} = 0 \qquad \text{on } \Gamma \times (0, t_{\text{final}}], \tag{2.2a}$$

$$\big(2\mu\boldsymbol{\varepsilon}(\boldsymbol{u}) - \psi\,\boldsymbol{I}\big)\boldsymbol{n} = \boldsymbol{0} \quad \text{and} \quad p = 0 \qquad \text{on } \Sigma \times (0, t_{\text{final}}], \tag{2.2b}$$

where the boundary $\partial\Omega = \Gamma \cup \Sigma$ is disjointly split into Γ and Σ where we prescribe clamped boundaries and zero fluid normal fluxes; and zero (total) traction together with constant fluid pressure, respectively. Homogeneity of the boundary conditions is only assumed to simplify the exposition of the analysis.

2.2 Weak formulation

In order to obtain a weak form (in space) for (2.1), we define the function spaces

$$\boldsymbol{V} := [H^1_\Gamma(\Omega)]^2,\ Q := H^1_\Sigma(\Omega),\ Z := L^2(\Omega).$$

Multiplying (2.1) by adequate test functions, integrating by parts (in space) whenever appropriate, and using the boundary conditions (2.2), leads to the following variational problem: For a given $t > 0$, find $\boldsymbol{u}(t) \in \boldsymbol{V}$, $p(t) \in Q$ and $\psi(t) \in Z$ such that

$$\begin{aligned} a_1(\boldsymbol{u},\boldsymbol{v}) \qquad\qquad &+ \quad b_1(\boldsymbol{v},\psi) = F(\boldsymbol{v}) \quad \forall \boldsymbol{v} \in \boldsymbol{V}, && (2.3a)\\ \tilde{a}_2(\partial_t p, q) + \qquad a_2(p,q) &- b_2(q,\,\partial_t\psi) = G(q) \quad \forall q \in Q, && (2.3b)\\ b_1(\boldsymbol{u},\phi) + b_2(p,\phi) &- \quad a_3(\psi,\phi) = \quad 0 \quad \forall \phi \in Z, && (2.3c)\end{aligned}$$

where the bilinear forms $a_1 : \boldsymbol{V} \times \boldsymbol{V} \to \mathbb{R}$, $a_2 : Q \times Q \to \mathbb{R}$, $a_3 : Z \times Z \to \mathbb{R}$, $b_1 : \boldsymbol{V} \times Z \to \mathbb{R}$, $b_2 : Q \times Z \to \mathbb{R}$, and linear functionals $F : \boldsymbol{V} \to \mathbb{R}$, $G : Q \to \mathbb{R}$, are given by the following expressions:

$$\begin{aligned} &a_1(\boldsymbol{u},\boldsymbol{v}) := 2\mu \int_\Omega \boldsymbol{\varepsilon}(\boldsymbol{u}) : \boldsymbol{\varepsilon}(\boldsymbol{v}), \quad b_1(\boldsymbol{v},\phi) := -\int_\Omega \phi \operatorname{div} \boldsymbol{v}, \quad F(\boldsymbol{v}) := \int_\Omega \rho \boldsymbol{b} \cdot \boldsymbol{v},\\ &G(q) := \int_\Omega \ell\, q, \quad \tilde{a}_2(p,q) := \left(c_0 + \frac{\alpha^2}{\lambda}\right) \int_\Omega pq, \quad a_2(p,q) := \frac{1}{\eta}\int_\Omega \kappa \nabla p \cdot \nabla q, \qquad (2.4)\\ &b_2(p,\phi) := \frac{\alpha}{\lambda}\int_\Omega p\phi, \quad a_3(\psi,\phi) := \frac{1}{\lambda}\int_\Omega \psi\phi. \end{aligned}$$

2.3 Properties of the bilinear forms and linear functionals

We now list the continuity, coercivity, and inf-sup conditions for the variational forms in (2.4). These are employed in [45] to derive the well-posedness of the stationary form of (2.1).

First we have the bounds

$$\begin{aligned} a_1(\boldsymbol{u},\boldsymbol{v}) &\le 2\mu\|\boldsymbol{\varepsilon}(\boldsymbol{u})\|_0\|\boldsymbol{\varepsilon}(\boldsymbol{v})\|_0 \le C\|\boldsymbol{u}\|_1\|\boldsymbol{v}\|_1 && \text{for all } \boldsymbol{u},\boldsymbol{v} \in \boldsymbol{V},\\ b_1(\boldsymbol{v},\phi) &\le \|\operatorname{div} \boldsymbol{v}\|_0\|\phi\|_0 \le C\|\boldsymbol{v}\|_1\|\phi\|_0 && \text{for all } \boldsymbol{v} \in \boldsymbol{V} \text{ and } \phi \in Z,\\ a_2(p,q) &\le \frac{\kappa_{\max}}{\eta}|p|_1|q|_1 \le \frac{\kappa_{\max}}{\eta}\|p\|_1\|q\|_1 && \text{for all } p,q \in Q,\\ b_2(q,\phi) &\le \frac{\alpha}{\lambda}\|q\|_0\|\phi\|_0, \quad a_3(\psi,\phi) \le \frac{1}{\lambda}\|\psi\|_0\|\phi\|_0 && \text{for all } q \in Q \text{ and } \psi,\phi \in Z,\\ F(\boldsymbol{v}) &\le \rho\|\boldsymbol{b}\|_0\|\boldsymbol{v}\|_1, \quad G(q) \le \|\ell\|_0\|q\|_0 && \text{for all } \boldsymbol{v} \in \boldsymbol{V} \text{ and } q \in Q, \end{aligned}$$

along with the coercivity of the diagonal bilinear forms, i.e.,

$$\begin{aligned} a_1(\boldsymbol{v},\boldsymbol{v}) &= 2\mu\|\boldsymbol{\varepsilon}(\boldsymbol{v})\|_0^2 \ge C\|\boldsymbol{v}\|_1^2 && \text{for all } \boldsymbol{v} \in \boldsymbol{V},\\ a_2(q,q) &\ge \frac{\kappa_{\min}}{\eta}\|q\|_1^2 && \text{for all } q \in Q,\\ a_3(\phi,\phi) &= \frac{1}{\lambda}\|\phi\|_0^2 && \text{for all } \phi \in Z, \end{aligned}$$

and the following inf-sup condition: there exists a constant $\beta > 0$ such that

$$\sup_{\boldsymbol{v}(\neq 0)\in \boldsymbol{V}} \frac{b_1(\boldsymbol{v},\phi)}{\|\boldsymbol{v}\|_1} \ge \beta\|\phi\|_0 \quad \text{for all } \phi \in Z.$$

The solvability of the continuous problem is not the focus here, and we refer to [48] for the corresponding well-posedness and regularity results.

3 Virtual element approximation

3.1 Discrete spaces and degrees of freedom

In this section we construct a VEM associated with (2.3). We start denoting by $\{\mathcal{T}_h\}_h$ a sequence of partitions of the domain Ω into general polygons K (open and simply connected sets whose boundary ∂K is a non-intersecting poly-line consisting of a finite number of straight line segments) having diameter h_K, and define as meshsize $h := \max_{K\in\mathcal{T}_h} h_K$. By N_K^v we denote the number of vertices in the polygon K, N_K^e stands for the number of edges on ∂K, and e is a generic edge of $\mathcal{T}_h$. For all $e \in \partial K$, we denote by $\boldsymbol{n}_K^e$ the unit normal pointing outwards K and by $\boldsymbol{t}_K^e$ the unit tangent vector along e on K, and V_i represents the i^{th} vertex of the polygon K.

As in [9] we need to assume regularity of the polygonal meshes in the following sense: there exists $C_{\mathcal{T}} > 0$ such that, for every h and every $K \in \mathcal{T}_h$, the ratio between the shortest edge and h_K is larger than $C_{\mathcal{T}}$; and $K \in \mathcal{T}_h$ is star-shaped with respect to every point within a ball of radius $C_{\mathcal{T}} h_K$.

Denoting by $\mathbb{P}_k(K)$ the space of polynomials of degree up to k, defined locally on $K \in \mathcal{T}_h$, we proceed to characterise the scalar energy projection operator $\Pi_K^\nabla : H^1(K) \to \mathbb{P}_1(K)$ by the relations

$$\left(\nabla(\Pi_K^\nabla q - q), \nabla r\right)_{0,K} = 0, \qquad P_K^0(\Pi_K^\nabla q - q) = 0, \tag{3.1}$$

valid for all $q \in H^1(K)$ and $r \in \mathbb{P}_1(K)$, and where $(\cdot,\cdot)_{0,K}$ denotes the L^2-product on K, and

$$P_K^0(q) := \int_{\partial K} q \,\mathrm{d}s.$$

If we now denote by $\mathcal{M}_k(K)$ the space of monomials of degree up to k, defined locally on $K \in \mathcal{T}_h$, we can define, on each polygon $K \in \mathcal{T}_h$, the local virtual element spaces for displacement, fluid pressure, and total pressure, as

$$\begin{aligned}
\boldsymbol{V}_h(K) &:= \left\{ \boldsymbol{v}_h \in [H^1(K)]^2 : \boldsymbol{v}_h|_{\partial K} \in \mathbb{B}(\partial K), \quad \begin{cases} -\Delta \boldsymbol{v}_h - \nabla s = \boldsymbol{0} \text{ in } K, \\ \operatorname{div} \boldsymbol{v}_h \in \mathbb{P}_0(K) \end{cases} \quad \text{for some } s \in L_0^2(K) \right\}, \\
Q_h(K) &:= \big\{ q_h \in H^1(K) \cap C^0(\partial K) : \ q_h|_e \in \mathbb{P}_1(e), \forall e \in \partial K, \\
&\qquad\qquad \Delta q_h|_K \in \mathbb{P}_1(K),\ (\Pi_K^\nabla q_h - q_h, m_\alpha)_{0,K} = 0 \ \forall m_\alpha \in \mathcal{M}_1(K) \big\}, \\
Z_h(K) &:= \mathbb{P}_0(K),
\end{aligned} \tag{3.2}$$

where we define

$$\mathbb{B}(\partial K) := \big\{ \boldsymbol{v}_h \in [C^0(\partial K)]^2 : \boldsymbol{v}_h|_e \cdot \boldsymbol{t}_K^e \in \mathbb{P}_1(e), \boldsymbol{v}_h|_e \cdot \boldsymbol{n}_K^e \in \mathbb{P}_2(e), \forall e \in \partial K \big\}.$$

It is clear from the above definitions that the dimension of $\boldsymbol{V}_h(K)$ is $3N_K^e$, the dimension of $Q_h(K)$ is N_K^v, and that of $Z_h(K)$ is one. Note that the virtual element space of degree $k = 1$, introduced in [1], has been utilised here for the approximation of fluid pressure. This facilitates the computation of the L^2-projection onto the space of polynomials of degree up to 1 (which are required in order to define the zero-order discrete bilinear form on $Q_h(K)$). Next, and in order to take advantage of the features of VEM discretisations (for instance, estimation of the terms of the discrete formulation without explicit computation of basis functions), we need to specify the degrees of freedom associated with (3.2). These entities will consist of discrete functionals of the type (taking as an example the space for total pressure)

$$(D_i) : Z_{h|K} \to \mathbb{R}; \qquad Z_{h|K} \ni \phi \mapsto D_i(\phi),$$

and we start with the degrees of freedom for the local displacement space $\boldsymbol{V}_h(K)$:

– $(D_v 1)$ the values of a discrete displacement $\boldsymbol{v}_h$ at vertices of the element;

– $(D_v 2)$ the normal displacement $\boldsymbol{v}_h \cdot \boldsymbol{n}_K^e$ at the mid-point of each edge $e \in \partial K$.

Then we precise the degrees of freedom for the local fluid pressure space $Q_h(K)$:

– (D_q) the values of q_h at vertices of the polygonal element.

And similarly, the degree of freedom for the local total pressure space $Z_h(K)$:

– (D_z) the value of ϕ_h over K.

It has been proven elsewhere (see e.g. [1, 5, 9]) that these degrees of freedom are unisolvent in their respective spaces. We also define global counterparts of the local virtual element spaces as follows:

$$\begin{aligned}
\boldsymbol{V}_h &:= \{\boldsymbol{v}_h \in \boldsymbol{V} : \boldsymbol{v}_h|_K \in \boldsymbol{V}_h(K)\ \forall K \in \mathcal{T}_h\}, \\
Q_h &:= \{q_h \in Q : q_h|_K \in Q_h(K)\ \forall K \in \mathcal{T}_h\}, \\
Z_h &:= \{\phi_h \in Z : \phi_h|_K \in Z_h(K)\ \forall K \in \mathcal{T}_h\}.
\end{aligned}$$

In addition, we denote by N^V the number of degrees of freedom for $\boldsymbol{V}_h$, by N^Q the number of degrees of freedom for Q_h, and by $\mathrm{dof}_r(s)$ the r-th degree of a given function s.

3.2 Projection operators

Besides (3.1) we need to define other projectors. Regarding restricted quantities, and in particular, bilinear forms restricted locally to a single element, we will use the notation $\mathcal{B}^K(\cdot,\cdot) = \mathcal{B}(\cdot,\cdot)|_K$ for a generic bilinear form $\mathcal{B}(\cdot,\cdot)$. Then we can define the energy projection $\boldsymbol{\Pi}_K^{\boldsymbol{\varepsilon}} : \boldsymbol{V}_h(K) \to [\mathbb{P}_1(K)]^2$ such that

$$\begin{aligned}
a_1^K(\boldsymbol{\Pi}_K^{\boldsymbol{\varepsilon}}\boldsymbol{v} - \boldsymbol{v}, \boldsymbol{r}) &= 0 \quad \text{for all } \boldsymbol{v} \in \boldsymbol{V}_h(K) \text{ and } \boldsymbol{r} \in [\mathbb{P}_1(K)]^2, \\
m^K(\boldsymbol{\Pi}_K^{\boldsymbol{\varepsilon}}\boldsymbol{v} - \boldsymbol{v}, \boldsymbol{r}) &= 0 \quad \text{for all } \boldsymbol{r} \in \ker(a_1^K(\cdot,\cdot)),
\end{aligned}$$

where

$$m^K(\boldsymbol{v}, \boldsymbol{r}) := \frac{1}{N_K^v} \sum_{i=1}^{N_K^v} \boldsymbol{v}(V_i) \cdot \boldsymbol{r}(V_i).$$

Then, using the degree of freedom $(D_v 1)$, we can readily compute the bilinear form $m^K(\boldsymbol{v}, \boldsymbol{r})$ for all $\boldsymbol{r} \in \ker(a_1^K(\cdot,\cdot))$ and $\boldsymbol{v} \in \boldsymbol{V}_h(K)$.

Next, for all $\boldsymbol{v} \in \boldsymbol{V}_h(K)$ let us consider the localised form

$$a_1^K(\boldsymbol{v}, \boldsymbol{r}) = \int_K \boldsymbol{\varepsilon}(\boldsymbol{v}) : \boldsymbol{\varepsilon}(\boldsymbol{r}) = -\int_K \boldsymbol{v} \cdot \mathbf{div}\big(\boldsymbol{\varepsilon}(\boldsymbol{r})\big) + \int_{\partial K} \boldsymbol{v} \cdot \big(\boldsymbol{\varepsilon}(\boldsymbol{r})\boldsymbol{n}_K^e\big)\,\mathrm{d}s.$$

One readily sees that $\mathbf{div}(\boldsymbol{\varepsilon}(\boldsymbol{r})) = \mathbf{0}$ and $\boldsymbol{\varepsilon}(\boldsymbol{r})$ is constant for all $\boldsymbol{r} \in [\mathbb{P}_1(K)]^2$. Therefore the other term can be simply rewritten as [12]

$$\int_{\partial K} \boldsymbol{v} \cdot \big(\boldsymbol{\varepsilon}(\boldsymbol{r})\boldsymbol{n}_K^e\big)\,\mathrm{d}s = \sum_{e \in \partial K} \left\{ \big(\boldsymbol{\varepsilon}(\boldsymbol{r})\boldsymbol{n}_K^e \cdot \boldsymbol{t}_K^e\big) \int_e (\boldsymbol{v} \cdot \boldsymbol{t}_K^e) + \big(\boldsymbol{\varepsilon}(\boldsymbol{r})\boldsymbol{n}_K^e \cdot \boldsymbol{n}_K^e\big) \int_e (\boldsymbol{v} \cdot \boldsymbol{n}_K^e) \right\}. \tag{3.3}$$

We can compute the first term on the right-hand side of (3.3) using the degree of freedom $(D_v 1)$ in conjunction with the trapezoidal rule, whereas for the second term it suffices to use the degrees of freedom $(D_v 1)$ and $(D_v 2)$ together with a Gauss-Lobatto quadrature. Thus, $\boldsymbol{\Pi}_K^{\boldsymbol{\varepsilon}}$ is computable on $\boldsymbol{V}_h(K)$.

We now define the L^2-projection on the scalar space as $\mathit{\Pi}^0_K : L^2(K) \to \mathbb{P}_1(K)$ such that

$$(\mathit{\Pi}^0_K q - q, r)_{0,K} = 0, \quad q \in L^2(K), r \in \mathbb{P}_1(K),$$

and we can clearly verify that $\mathit{\Pi}^0_K q_h = \mathit{\Pi}^\nabla_K q_h,\ \forall q_h \in Q_h$.

Finally, we consider the L^2-projection onto the piecewise constant functions, $\mathit{\Pi}^{0,0}_K : L^2(K) \to \mathbb{P}_0(K)$ and $\boldsymbol{\mathit{\Pi}}^{0,0}_K : [L^2(K)]^2 \to [\mathbb{P}_0(K)]^2$, for scalar and vector fields, respectively. We observe that the latter is fully computable on the virtual space $\boldsymbol{V}_h(K)$ [13].

3.3 Discrete bilinear forms and formulations

For all $\boldsymbol{u}_h, \boldsymbol{v}_h \in \boldsymbol{V}_h(K)$ and $p_h, q_h \in Q_h(K)$ we now define the local discrete bilinear forms

$$\begin{aligned}
a_1^h(\boldsymbol{u}_h, \boldsymbol{v}_h)|_K &:= a_1^K(\boldsymbol{\mathit{\Pi}}^{\boldsymbol{\varepsilon}}_K \boldsymbol{u}_h, \boldsymbol{\mathit{\Pi}}^{\boldsymbol{\varepsilon}}_K \boldsymbol{v}_h) + S_1^K\big((\boldsymbol{I} - \boldsymbol{\mathit{\Pi}}^{\boldsymbol{\varepsilon}}_K)\boldsymbol{u}_h, (\boldsymbol{I} - \boldsymbol{\mathit{\Pi}}^{\boldsymbol{\varepsilon}}_K)\boldsymbol{v}_h\big),\\
a_2^h(p_h, q_h)|_K &:= a_2^K(\mathit{\Pi}^\nabla_K p_h, \mathit{\Pi}^\nabla_K q_h) + S_2^K\big((I - \mathit{\Pi}^\nabla_K)p_h, (I - \mathit{\Pi}^\nabla_K)q_h\big),\\
\tilde{a}_2^h(p_h, q_h)|_K &:= \tilde{a}_2^K(\mathit{\Pi}^0_K p_h, \mathit{\Pi}^0_K q_h) + S_0^K\big((I - \mathit{\Pi}^0_K)p_h, (I - \mathit{\Pi}^0_K)q_h\big),
\end{aligned}$$

where the stabilisation of the bilinear forms $S_1^K(\cdot,\cdot), S_2^K(\cdot,\cdot), S_0^K(\cdot,\cdot)$ acting on the kernel of their respective operators $\boldsymbol{\mathit{\Pi}}^{\boldsymbol{\varepsilon}}_K,\ \mathit{\Pi}^\nabla_K,\ \mathit{\Pi}^0_K$, is defined as

$$\begin{aligned}
S_1^K(\boldsymbol{u}_h, \boldsymbol{v}_h) &:= \sigma_1^K \sum_{l=1}^{N^V} \mathrm{dof}_l(\boldsymbol{u}_h)\mathrm{dof}_l(\boldsymbol{v}_h), \quad \boldsymbol{u}_h, \boldsymbol{v}_h \in \ker(\boldsymbol{\mathit{\Pi}}^{\boldsymbol{\varepsilon}}_K);\\
S_2^K(p_h, q_h) &:= \sigma_2^K \sum_{l=1}^{N^Q} \mathrm{dof}_l(p_h)\mathrm{dof}_l(q_h), \quad p_h, q_h \in \ker(\mathit{\Pi}^\nabla_K);\\
S_0^K(p_h, q_h) &:= \sigma_0^K \mathrm{area}(K) \sum_{l=1}^{N^Q} \mathrm{dof}_l(p_h)\mathrm{dof}_l(q_h), \quad p_h, q_h \in \ker(\mathit{\Pi}^0_K),
\end{aligned}$$

respectively, where σ_1^K, σ_2^K and σ_0^K are positive multiplicative factors to take into account the magnitude of the physical parameters (independent of a mesh size).

Note that for all $\boldsymbol{v}_h \in \boldsymbol{V}_h(K),\ q_h \in Q_h(K)$, these stabilising terms satisfy the following relations (see, e.g., [5, 12])

$$\begin{aligned}
\alpha_* a_1^K(\boldsymbol{v}_h, \boldsymbol{v}_h) \le S_1^K(\boldsymbol{v}_h, \boldsymbol{v}_h) \le \alpha^* a_1^K(\boldsymbol{v}_h, \boldsymbol{v}_h),\\
\zeta_* a_2^K(q_h, q_h) \le S_2^K(q_h, q_h) \le \zeta^* a_2^K(q_h, q_h),\\
\tilde{\zeta}_* \tilde{a}_2^K(q_h, q_h) \le S_0^K(q_h, q_h) \le \tilde{\zeta}^* \tilde{a}_2^K(q_h, q_h),
\end{aligned} \tag{3.4}$$

where $\alpha_*, \alpha^*, \zeta_*, \zeta^*, \tilde{\zeta}_*, \tilde{\zeta}^*$ are positive constants independent of K and h_K. Now, for all $\boldsymbol{u}_h, \boldsymbol{v}_h \in \boldsymbol{V}_h,\ p_h, q_h \in Q_h$, the global discrete bilinear forms are specified as

$$\begin{aligned}
a_1^h(\boldsymbol{u}_h, \boldsymbol{v}_h) &:= \sum_{K \in \mathcal{T}_h} a_1^h(\boldsymbol{u}_h, \boldsymbol{v}_h)|_K, \quad a_2^h(p_h, q_h) := \sum_{K \in \mathcal{T}_h} a_2^h(p_h, q_h)|_K,\\
\tilde{a}_2^h(p_h, q_h) &:= \sum_{K \in \mathcal{T}_h} \tilde{a}_2^h(p_h, q_h)|_K, \quad b_1(\boldsymbol{v}_h, \phi_h) := \sum_{K \in \mathcal{T}_h} b_1^K(\boldsymbol{v}_h, \phi_h),\\
a_3(\psi_h, \phi_h) &:= \sum_{K \in \mathcal{T}_h} a_3^K(\psi_h, \phi_h), \quad b_2(q_h, \phi_h) := \sum_{K \in \mathcal{T}_h} b_2^K(q_h, \phi_h).
\end{aligned}$$

In addition, we observe that

$$b_2(p_h, \phi_h) = \frac{\alpha}{\lambda} \sum_{K \in \mathcal{T}_h} \int_K p_h \phi_h = \frac{\alpha}{\lambda} \sum_{K \in \mathcal{T}_h} \int_K \mathit{\Pi}^0_K p_h \phi_h. \tag{3.5}$$

On the other hand, the discrete linear functionals, defined on each element K, are

$$F^h(\boldsymbol{v}_h)|_K := \rho \int_K \boldsymbol{b}_h(\cdot,t)\cdot\boldsymbol{v}_h, \quad \boldsymbol{v}_h \in \boldsymbol{V}_h; \quad G^h(q_h)|_K := \int_K \ell_h(\cdot,t) q_h, \quad q_h \in Q_h,$$

where the discrete load and volumetric source are given by:

$$\boldsymbol{b}_h(\cdot,t)|_K := \boldsymbol{\Pi}_K^{0,0}\boldsymbol{b}(\cdot,t), \quad \ell_h(\cdot,t)|_K := \Pi_K^0 \ell(\cdot,t).$$

In view of (3.4), the discrete bilinear forms $a_1^h(\cdot,\cdot)$, $\tilde{a}_2^h(\cdot,\cdot)$ and $a_2^h(\cdot,\cdot)$ are coercive and bounded in the following manner [5, 9, 51]

$$\begin{aligned}
a_1^h(\boldsymbol{u}_h,\boldsymbol{u}_h) &\geq \min\{1,\alpha_*\}\, 2\mu\, \|\boldsymbol{\varepsilon}(\boldsymbol{u}_h)\|_0^2 && \text{for all } \boldsymbol{u}_h \in \boldsymbol{V}_h,\\
a_2^h(q_h,q_h) &\geq \min\{1,\zeta_*\}\, \frac{\kappa_{\min}}{\eta}\, \|\nabla q_h\|_0^2 && \text{for all } q_h \in Q_h,\\
\tilde{a}_2^h(q_h,q_h) &\geq \min\{1,\tilde{\zeta}_*\}\left(c_0 + \frac{\alpha^2}{\lambda}\right) \|q_h\|_0^2 && \text{for all } q_h \in Q_h,\\
a_1^h(\boldsymbol{u}_h,\boldsymbol{v}_h) &\leq \max\{1,\alpha^*\}\, 2\mu\, \|\boldsymbol{\varepsilon}(\boldsymbol{u}_h)\|_0 \|\boldsymbol{\varepsilon}(\boldsymbol{v}_h)\|_0 && \text{for all } \boldsymbol{u}_h,\boldsymbol{v}_h \in \boldsymbol{V}_h,\\
a_2^h(p_h,q_h) &\leq \max\{1,\zeta^*\}\, \frac{\kappa_{\max}}{\eta}\, \|\nabla p_h\|_0 \|\nabla q_h\|_0 && \text{for all } p_h,q_h \in Q_h,\\
\tilde{a}_2^h(p_h,q_h) &\leq \max\{1,\tilde{\zeta}^*\}\left(c_0 + \frac{\alpha^2}{\lambda}\right) \|p_h\|_0\|q_h\|_0 && \text{for all } p_h,q_h \in Q_h.
\end{aligned}$$

Moreover, by using definitions of the operators $\boldsymbol{\Pi}_K^{0,0}$ and Π_K^0, we may deduce that the following bounds hold for the linear functionals:

$$\begin{aligned}
F^h(\boldsymbol{v}_h) &\leq \rho\|\boldsymbol{b}\|_0\|\boldsymbol{v}_h\|_0 && \text{for all } \boldsymbol{v}_h \in \boldsymbol{V}_h,\\
G^h(q_h) &\leq \|\ell\|_0\|q_h\|_0 && \text{for all } q_h \in Q_h.
\end{aligned}$$

We also recall that the bilinear form $b_1(\cdot,\cdot)$ satisfies the following discrete inf-sup condition on $\boldsymbol{V}_h \times Z_h$: there exists $\tilde{\beta} > 0$, independent of h, such that (see [5]),

$$\sup_{\boldsymbol{v}_h(\neq 0)\in\boldsymbol{V}_h} \frac{b_1(\boldsymbol{v}_h,\phi_h)}{\|\boldsymbol{v}_h\|_1} \geq \tilde{\beta}\|\phi_h\|_0 \quad \text{for all } \phi_h \in Z_h. \tag{3.6}$$

The semidiscrete virtual element formulation is now defined as follows: For all $t > 0$, given $\boldsymbol{u}_h(0)$, $p_h(0)$, $\psi_h(0)$, find $\boldsymbol{u}_h \in \boldsymbol{L}^2((0,t_{\text{final}}],\boldsymbol{V}_h)$, $p_h \in L^2((0,t_{\text{final}}],Q_h)$, $\psi_h \in L^2((0,t_{\text{final}}],Z_h)$ with $\partial_t p_h \in L^2((0,t_{\text{final}}],Q_h)$, $\partial_t\psi_h \in L^2((0,t_{\text{final}}],Z_h)$ such that

$$a_1^h(\boldsymbol{u}_h,\boldsymbol{v}_h) + b_1(\boldsymbol{v}_h,\psi_h) = F^h(\boldsymbol{v}_h) \quad \forall \boldsymbol{v}_h \in \boldsymbol{V}_h, \tag{3.7a}$$

$$\tilde{a}_2^h(\partial_t p_h,q_h) + a_2^h(p_h,q_h) - b_2(q_h,\partial_t\psi_h) = G^h(q_h) \quad \forall q_h \in Q_h, \tag{3.7b}$$

$$b_1(\boldsymbol{u}_h,\phi_h) + b_2(p_h,\phi_h) - a_3(\psi_h,\phi_h) = 0 \quad \forall \phi_h \in Z_h. \tag{3.7c}$$

The following result will be used for proving the stability and establishing the error estimates for the semi-discrete scheme without employing the Gronwall's inequality. For a detailed proof, we refer to [37, Lemma 3.2].

Lemma 3.1 *Let $X(t)$ be a continuous function, and consider the non-negative functions $F(t)$ and $D(t)$ satisfying, for constants $C_0 \geq 1$ and $C_1 > 0$, the bound*

$$X^2(t) \leq C_0X^2(0) + C_1X(0) + D(t) + \int_0^t F(s)X(s)\,\mathrm{d}s, \quad \forall\, t \in [0,t_{\text{final}}].$$

Then, for each $t \in [0,t_{\text{final}}]$, there holds

$$X(t) \lesssim X(0) + \max\left\{C_1 + \int_0^t F(s)\,\mathrm{d}s,\; D(t)^{1/2}\right\}. \tag{3.8}$$

Note that squaring both sides of (3.8) and using Cauchy–Schwarz inequality, we can rewrite (3.8) in the following manner

$$X(t)^2 \lesssim X(0)^2 + \max\left\{C_1^2 + \int_0^t F(s)^2\,\mathrm{d}s,\ D(t)\right\}. \tag{3.9}$$

Now we establish the stability of (3.7).

Theorem 3.1 (Stability of the semi-discrete problem) *Let $(\boldsymbol{u}_h(t), p_h(t), \psi_h(t))$ be a solution of (3.7) for each $t \in (0, t_{\text{final}}]$. Then there exists a constant $C > 0$ independent of c_0, λ, and h, such that*

$$\begin{aligned}
&\mu\|\boldsymbol{\varepsilon}(\boldsymbol{u}_h(t))\|_0^2 + c_0\|p_h(t)\|_0^2 + \|\psi_h(t)\|_0^2 + \frac{\kappa_{\min}}{\eta}\int_0^t \|\nabla p_h(s)\|_0^2\,\mathrm{d}s \\
&\leq C\Big(\mu\|\boldsymbol{\varepsilon}(\boldsymbol{u}_h(0))\|_0^2 + \Big(c_0 + \frac{\alpha^2}{\lambda}\Big)\|p_h(0)\|_0^2 + \frac{1}{\lambda}\|\psi_h(0)\|_0^2 + \int_0^t \|\partial_t \boldsymbol{b}(s)\|_0^2\,\mathrm{d}s \\
&\qquad + \sup_{t\in[0,t_{final}]}\|\boldsymbol{b}(t)\|_0^2 + \int_0^t \|\ell(s)\|_0^2\,\mathrm{d}s\Big).
\end{aligned} \tag{3.10}$$

Proof. Following [37], we can differentiate equation (3.7c) with respect to time and choose as test function $\phi_h = -\psi_h$. We get

$$-b_1(\partial_t \boldsymbol{u}_h, \psi_h) - b_2(\partial_t p_h, \psi_h) + a_3(\partial_t \psi_h, \psi_h) = 0.$$

Then we take $q_h = p_h$ in (3.7b), $\boldsymbol{v}_h = \partial_t \boldsymbol{u}_h$ in (3.7a) and add the result to the previous relation to obtain

$$\begin{aligned}
&a_1^h(\boldsymbol{u}_h, \partial_t \boldsymbol{u}_h) + b_1(\partial_t \boldsymbol{u}_h, \psi_h) + \tilde{a}_2^h(\partial_t p_h, p_h) + a_2^h(p_h, p_h) - b_2(p_h, \partial_t \psi_h) \\
&- b_1(\partial_t \boldsymbol{u}_h, \psi_h) - b_2(\partial_t p_h, \psi_h) + a_3(\partial_t \psi_h, \psi_h) = F^h(\partial_t \boldsymbol{u}_h) + G^h(p_h).
\end{aligned}$$

Using the stability of the bilinear forms $a_1^h(\cdot,\cdot)$, $a_2^h(\cdot,\cdot)$, $S_0^K(\cdot,\cdot)$ as well as the definition of the discrete bilinear forms $b_1(\cdot,\cdot)$ (cf. (3.5)) and $\tilde{a}_2^h(\cdot,\cdot)$, we readily have

$$\begin{aligned}
&\frac{\mu}{2}\frac{\mathrm{d}}{\mathrm{d}t}\|\boldsymbol{\varepsilon}(\boldsymbol{u}_h)\|_0^2 + \frac{c_0}{2}\frac{\mathrm{d}}{\mathrm{d}t}\|p_h\|_0^2 + \frac{\kappa_{\min}}{\eta}\|\nabla p_h\|_0^2 + \frac{1}{\lambda}\|\psi_h\|_{0,K}^2 \\
&+ \sum_K\Bigg(\frac{\alpha^2}{\lambda}\Big(\big(\partial_t(\Pi_K^0 p_h), \Pi_K^0 p_h\big)_{0,K} + S_0^K\big((I-\Pi_K^0)\partial_t p_h, (I-\Pi_K^0)p_h\big)\Big) \\
&\qquad - \frac{\alpha}{\lambda}\Big((\Pi_K^0 p_h, \partial_t\psi_h)_{0,K} + \big(\partial_t(\Pi_K^0 p_h), \psi_h\big)_{0,K}\Big)\Bigg) \\
&\lesssim F^h(\partial_t \boldsymbol{u}_h) + G^h(p_h).
\end{aligned} \tag{3.11}$$

Rearranging terms on the left-hand side gives

$$\begin{aligned}
&\frac{\mu}{2}\frac{\mathrm{d}}{\mathrm{d}t}\|\boldsymbol{\varepsilon}(\boldsymbol{u}_h)\|_0^2 + \frac{\kappa_{\min}}{\eta}\|\nabla p_h\|_0^2 + \frac{c_0}{2}\frac{\mathrm{d}}{\mathrm{d}t}\|p_h\|_0^2 \\
&+ \frac{1}{\lambda}\sum_K\Bigg(\big(\partial_t(\alpha\Pi_K^0 p_h - \psi_h), (\alpha\Pi_K^0 p_h - \psi_h)\big)_{0,K} \\
&\qquad + \frac{\alpha^2}{2}\frac{\mathrm{d}}{\mathrm{d}t}S_0^K\big((I-\Pi_K^0)p_h, (I-\Pi_K^0)p_h\big)\Bigg) \lesssim F^h(\partial_t \boldsymbol{u}_h) + G^h(p_h),
\end{aligned}$$

and after exploiting the stability of $S_0^K(\cdot,\cdot)$ and integrating from 0 to t, we arrive at

$$\mu\|\boldsymbol{\varepsilon}(\boldsymbol{u}_h(t))\|_0^2 + c_0\|p_h(t)\|_0^2 + \frac{\alpha^2}{\lambda}\sum_K\|(I-\Pi_K^0)p_h(t)\|_{0,K}^2$$

$$
\begin{aligned}
&+\frac{1}{\lambda}\sum_K \|(\alpha\varPi_K^0 p_h-\psi_h)(t)\|_{0,K}^2+\frac{\kappa_{\min}}{\eta}\int_0^t \|\nabla p_h(s)\|_0^2\,\mathrm{d}s\\
\le&\mu\|\boldsymbol{\varepsilon}(\boldsymbol{u}_h(0))\|_0^2+c_0\|p_h(0)\|_0^2\\
&+\frac{\alpha^2}{\lambda}\sum_K \|(I-\varPi_K^0)p_h(0)\|_{0,K}^2+\frac{1}{\lambda}\sum_K \|(\alpha\varPi_K^0 p_h-\psi_h)(0)\|_{0,K}^2\\
&+C\Bigg(\underbrace{\rho\int_0^t\sum_K\big(\boldsymbol{b}(s),\boldsymbol{\varPi}_K^{0,0}\partial_t\boldsymbol{u}_h(s)\big)_{0,K}\,\mathrm{d}s}_{=:T_1}+\underbrace{\int_0^t\sum_K\big(\ell(s),\varPi_K^0 p_h(s)\big)_{0,K}\,\mathrm{d}s}_{=:T_2}\Bigg).
\end{aligned}
$$

Then, integrating by parts (with respect to time) and applying the Korn, Poincaré, and Young inequalities implies that

$$
\begin{aligned}
T_1&=\rho\sum_K\Big(\big(\boldsymbol{b}(t),\boldsymbol{\varPi}_K^{0,0}\boldsymbol{u}_h(t)\big)_{0,K}-\big(\boldsymbol{b}(0),\boldsymbol{\varPi}_K^{0,0}\boldsymbol{u}_h(0)\big)_{0,K}\Big)\\
&\qquad-\rho\int_0^t\sum_K\big(\partial_t\boldsymbol{b}(s),\boldsymbol{\varPi}_K^{0,0}\boldsymbol{u}_h(s)\big)_{0,K}\,\mathrm{d}s\\
&\le\mu\|\boldsymbol{\varepsilon}(\boldsymbol{u}_h(t))\|_0^2+C_1\rho\left(\frac{\rho}{\mu}\|\boldsymbol{b}(t)\|_0^2+\|\boldsymbol{b}(0)\|_0\|\boldsymbol{\varepsilon}(\boldsymbol{u}_h(0))\|_0+\int_0^t\|\partial_t\boldsymbol{b}(s)\|_0\|\boldsymbol{\varepsilon}(\boldsymbol{u}_h(s))\|_0\,\mathrm{d}s\right).
\end{aligned}
$$

In turn, the bound for T_2 follows from the Cauchy-Schwarz, Poincaré, and Young inequalities in the following manner:

$$
\begin{aligned}
T_2&=\int_0^t\sum_K(\ell(s),\varPi_K^0 p_h(s))_{0,K}\,\mathrm{d}s\\
&\le\int_0^t\|\ell(s)\|_0\|p_h(s)\|_0\,\mathrm{d}s\le C_2\frac{\eta}{\kappa_{\min}}\int_0^t\|\ell(s)\|_0^2\,\mathrm{d}s+\frac{\kappa_{\min}}{2\eta}\int_0^t\|\nabla p_h(s)\|_0^2\,\mathrm{d}s.
\end{aligned}
$$

Thus, we achieve

$$
\begin{aligned}
&\mu\|\boldsymbol{\varepsilon}(\boldsymbol{u}_h(t))\|_0^2+c_0\|p_h(t)\|_0^2+\frac{\alpha^2}{\lambda}\sum_K\|(I-\varPi_K^0)p_h(t)\|_{0,K}^2\\
&\qquad+\frac{1}{\lambda}\sum_K\|(\alpha\varPi_K^0p_h-\psi_h)(t)\|_{0,K}^2+\frac{\kappa_{\min}}{2\eta}\int_0^t\|\nabla p_h(s)\|_0^2\,\mathrm{d}s\\
\le&\mu\|\boldsymbol{\varepsilon}(\boldsymbol{u}_h(0))\|_0^2+c_0\|p_h(0)\|_0^2+\frac{\alpha^2}{\lambda}\sum_K\|(I-\varPi_K^0)p_h(0)\|_{0,K}^2\\
&\qquad+\frac{1}{\lambda}\sum_K\|(\alpha\varPi_K^0p_h-\psi_h)(0)\|_{0,K}^2+C\bigg(\int_0^t\|\ell(s)\|_0^2\,\mathrm{d}s+\Big(\|\boldsymbol{b}(t)\|_0^2\\
&\qquad\quad+\|\boldsymbol{b}(0)\|_0\|\boldsymbol{\varepsilon}(\boldsymbol{u}_h(0))\|_0+\int_0^t\|\partial_t\boldsymbol{b}(s)\|_0\|\boldsymbol{\varepsilon}(\boldsymbol{u}_h(s))\|_0\,\mathrm{d}s\Big)\bigg).
\end{aligned}
\tag{3.12}
$$

Let $X^2(t)$ denote the lower bound in the inequality (3.12) and choose $C_0=1$, $C_1=C\|\boldsymbol{b}(0)\|_0$, $F(t)=C\|\partial_t\boldsymbol{b}(t)\|_0$ and $D(t)=C(\|\boldsymbol{b}(t)\|_0^2+\int_0^t\|\ell(s)\|_0^2\,\mathrm{d}s)$ in Lemma 3.1. Then (3.9) enables us to write

$$
\begin{aligned}
&\mu\|\boldsymbol{\varepsilon}(\boldsymbol{u}_h(t))\|_0^2+c_0\|p_h(t)\|_0^2+\frac{\alpha^2}{\lambda}\sum_K\|(I-\varPi_K^0)p_h(t)\|_{0,K}^2\\
&\qquad+\frac{1}{\lambda}\sum_K\|(\alpha\varPi_K^0p_h-\psi_h)(t)\|_{0,K}^2+\frac{\kappa_{\min}}{2\eta}\int_0^t\|\nabla p_h(s)\|_0^2\,\mathrm{d}s
\end{aligned}
$$

$$\lesssim \mu\|\boldsymbol{\varepsilon}(\boldsymbol{u}_h(0))\|_0^2 + c_0\|p_h(0)\|_0^2 + \frac{\alpha^2}{\lambda}\sum_K \|(I-\Pi_K^0)p_h(0)\|_{0,K}^2 \tag{3.13}$$
$$+\frac{1}{\lambda}\sum_K \|(\alpha\Pi_K^0 p_h - \psi_h)(0)\|_{0,K}^2 + \|\boldsymbol{b}(t)\|_0^2 + \|\boldsymbol{b}(0)\|_0^2 + \int_0^t (\|\ell(s)\|_0^2 + \|\partial_t \boldsymbol{b}(s)\|_0^2)\,\mathrm{d}s.$$

On the other hand, the discrete inf-sup condition (3.6) along with (3.7a) gives

$$\|\psi_h\|_0 \le \sup_{\boldsymbol{v}_h(\neq 0)\in \boldsymbol{V}_h} \frac{1}{\|\boldsymbol{v}_h\|_1}\big(F^h(\boldsymbol{v}_h) - a_1^h(\boldsymbol{u}_h,\boldsymbol{v}_h)\big) \le C\big(\|\boldsymbol{b}\|_0 + \|\boldsymbol{\varepsilon}(\boldsymbol{u}_h)\|_0\big). \tag{3.14}$$

And then note that inequality (3.13) together with (3.14) concludes the proof of (3.10). Moreover, we observe from (3.12) that the generic constant C appearing in (3.10) is independent of c_0, λ. Therefore the proved stability remains valid even with $c_0 \to 0$, $\lambda \to \infty$. □

The energy estimates (3.10) help us in obtaining the following result.

Corollary 3.1 (Solvability of the discrete problem) *The problem (3.7) has a unique solution in $\boldsymbol{V}_h \times Q_h \times Z_h$ for each $t \in (0, t_{\text{final}}]$.*

Proof. Let $\boldsymbol{u}_h(t) := \sum_{i=1}^{N^{\boldsymbol{V}}} U_i(t)\xi_i$, $p_h(t) := \sum_{j=1}^{N^Q} P_j(t)\chi_j$, $\psi_h(t) := \sum_{l=1}^{N^Z} Z_l(t)\Phi_l$ where $\xi_i(1 \le i \le N^{\boldsymbol{V}})$, $\chi_j(1 \le j \le N^Q)$, $\Phi_l(1 \le l \le N^Z$, where N^Z coincides with the number of elements in $\mathcal{T}_h)$ are the basis functions for the spaces $\boldsymbol{V}_h, Q_h, Z_h$ respectively. Then (3.7) can be written as the following system of first-order differential equations:

$$\underbrace{\begin{pmatrix} \mathbf{0} & \mathbf{0} & \mathbf{0} \\ \mathbf{0} & \tilde{A}2 & -B2 \\ \mathbf{0} & \mathbf{0} & \mathbf{0} \end{pmatrix}}_{=:\mathcal{A}} \begin{pmatrix} \dot{U}(t) \\ \dot{P}(t) \\ \dot{Z}(t) \end{pmatrix} + \underbrace{\begin{pmatrix} A1 & \mathbf{0} & B1 \\ \mathbf{0} & A2 & \mathbf{0} \\ B1 & B2 & -A3 \end{pmatrix}}_{=:\mathcal{B}} \begin{pmatrix} U(t) \\ P(t) \\ Z(t) \end{pmatrix} = \begin{pmatrix} \boldsymbol{F}(t) \\ \boldsymbol{G}(t) \\ \mathbf{0} \end{pmatrix}. \tag{3.15}$$

In view of the classical theory of linear systems of differential equations, (3.15) possesses a unique solution if the matrix $\mathcal{A}+\mathcal{B}$ is invertible (see also [53]). To achieve this, we first rewrite the following problem corresponding to the matrix $\mathcal{A}+\mathcal{B}$: For $(L_1^h, L_2^h, L_3^h) \in \boldsymbol{V}_h' \times Q_h' \times Z_h'$, find $\boldsymbol{u}_h \in \boldsymbol{V}_h$, $p_h \in Q_h$, $q_h \in Z_h$ such that

$$a_1^h(\boldsymbol{u}_h,\boldsymbol{v}_h) \qquad\qquad + b_1(\boldsymbol{v}_h,\psi_h) = L_1^h(\boldsymbol{v}_h) \quad \forall \boldsymbol{v}_h \in \boldsymbol{V}_h, \tag{3.16a}$$
$$\tilde{a}_2^h(p_h,q_h) + \qquad a_2^h(p_h,q_h) - b_2(q_h,\psi_h) = L_2^h(q_h) \quad \forall q_h \in Q_h, \tag{3.16b}$$
$$b_1(\boldsymbol{u}_h,\phi_h) + b_2(p_h,\phi_h) - a_3(\psi_h,\phi_h) = L_3^h(\phi_h) \quad \forall \phi_h \in Z_h. \tag{3.16c}$$

Now, the unique solvability of (3.16) (and the invertibility of the matrix $\mathcal{A}+\mathcal{B}$) can be established by showing that the homogenous counterpart of system (3.16) has only the trivial solution. Setting to zero the functionals defining the right-hand side of (3.16), i.e., $L_1^h(\boldsymbol{v}_h) = L_2^h(q_h) = L_3^h(\phi_h) = 0$, and choosing $\boldsymbol{v}_h = \boldsymbol{u}_h, \phi_h = \psi_h, q_h = p_h$ in (3.16), we readily obtain the following bounds by proceeding in the similar fashion (using the coercivity of $a_1^h(\cdot,\cdot)$, $a_2^h(\cdot,\cdot)$, Young's inequality and definition of $\tilde{a}_2^h(\cdot,\cdot)$, $b_2(\cdot,\cdot)$, $a_3^h(\cdot,\cdot)$) as in the proof of (3.10)

$$\mu\|\boldsymbol{\varepsilon}(\boldsymbol{u}_h)\|_0^2 + \frac{\kappa_{\min}}{\eta}\|\nabla p_h\|_0^2 \le 0,$$

and hence an application of the Poincaré and Korn inequalities together with the inf-sup condition of $b_1(\cdot,\cdot)$ yields $\boldsymbol{u}_h = \mathbf{0}$, $p_h = 0$ and $\psi_h = 0$. □

Next, we discretise in time using the backward Euler method with the constant step size $\Delta t = t_{\text{final}}/N$ and denote any function f at $t = t_n$ by f^n. The fully discrete scheme reads:

Given $\boldsymbol{u}_h^0$, p_h^0, ψ_h^0, and for $t_n = n\Delta t$, $n = 1, \ldots, N$, find $\boldsymbol{u}_h^n \in \boldsymbol{V}_h$,

$p_h^n \in Q_h$ and $\psi_h^n \in Z_h$ such that for all $\boldsymbol{v}_h \in \boldsymbol{V}_h$, $q_h \in Q_h$ and $\phi_h \in Z_h$

$$a_1^h(\boldsymbol{u}_h^n, \boldsymbol{v}_h) + b_1(\boldsymbol{v}_h, \psi_h^n) = F^{h,n}(\boldsymbol{v}_h), \tag{3.17a}$$

$$\tilde{a}_2^h\left(p_h^n, q_h\right) + \Delta t a_2^h(p_h^n, q_h) - b_2\left(q_h, \psi_h^n\right) = \Delta t G^{h,n}(q_h) + \tilde{a}_2^h\left(p_h^{n-1}, q_h\right) - b_2\left(q_h, \psi_h^{n-1}\right), \tag{3.17b}$$

$$b_1(\boldsymbol{u}_h^n, \phi_h) + b_2(p_h^n, \phi_h) - a_3(\psi_h^n, \phi_h) = 0, \tag{3.17c}$$

where for all $\boldsymbol{v}_h \in \boldsymbol{V}_h$ and $q_h \in Q_h$ we define

$$F^{h,n}(\boldsymbol{v}_h)|_K := \rho \int_K \boldsymbol{b}_h(t^n) \cdot \boldsymbol{v}_h, \quad G^{h,n}(q_h)|_K := \int_K \ell_h(t^n) q_h.$$

With the aim of showing the stability and convergence of the fully-discrete scheme, we provide first the following auxiliary result. A proof, sketched below, follows similarly as in [36, Lemma 3.2].

Lemma 3.2 *Let X_n, $1 \leq n \leq N$ be a finite sequence of functions with non-negative constants C_0, C_1 and finite sequences D_n and G_n such that*

$$X_n^2 \leq C_0 X_0^2 + C_1 X_0 + D_n + \sum_{j=1}^n G_j X_j \quad \textit{for all } 1 \leq n \leq N.$$

Then there holds

$$X_n^2 \lesssim X_0^2 + \max\left\{C_1^2 + \sum_{j=1}^n G_j^2,\ D_n\right\} \quad \textit{for all } 1 \leq n \leq N. \tag{3.18}$$

Proof. It is sufficient to show that the relation holds for n, which is the smallest integer such that $X_n = \max_{1 \leq i \leq N} X_i$. There can be two possibilities, namely either (i) $C_1 X_0 + \sum_{j=1}^n G_j X_j \leq D_n$, or (ii) $D_n > C_1 X_0 + \sum_{j=1}^n G_j X_j$. In case (i), the bound (3.18) trivially holds. In case (ii), using the upper bound X_n and Young's inequality yields

$$\begin{aligned} X_n^2 &\leq C_0 X_0^2 + 2\left(C_1 X_0 + \sum_{j=1}^n G_j X_j\right) \lesssim \left(C_0 X_0 + 2\left(C_1 + \sum_{j=1}^n G_j\right)\right) X_n \\ &\leq \frac{1}{2}\left(C_0 X_0 + 2\left(C_1 + \sum_{j=1}^n G_j\right)\right)^2 + \frac{1}{2} X_n^2. \end{aligned}$$

Now taking the common term of X_n^2 together and squaring the remaining terms on the right-hand side completes the proof. □

Theorem 3.2 (Stability of the fully-discrete problem) *The unique solution to problem (3.17) depends continuously on data. More precisely, there exists a constant C independent of c_0, λ, h and Δt such that*

$$\begin{aligned} &\mu\|\boldsymbol{\varepsilon}(\boldsymbol{u}_h^n)\|_0^2 + c_0\|p_h^n\|_0^2 + \|\psi_h^n\|_0^2 + (\Delta t)\frac{\kappa_{\min}}{\eta}\sum_{j=1}^n \|\nabla p_h^j\|_0^2 \\ &\leq C\biggl(\mu\|\boldsymbol{\varepsilon}(\boldsymbol{u}_h^0)\|_0^2 + \left(c_0 + \frac{\alpha^2}{\lambda}\right)\|p_h^0\|_0^2 + \frac{1}{\lambda}\|\psi_h^0\|_0^2 + \max_{0\leq j\leq n}\|\boldsymbol{b}^j\|_0^2 \\ &\qquad + (\Delta t)\sum_{j=1}^n\left(\|\partial_t \boldsymbol{b}^j\|_0^2 + \|\ell^j\|_0^2\right) + (\Delta t)^2\int_0^T \|\partial_{tt}\boldsymbol{b}(s)\|_0^2 \,\mathrm{d}s\biggr), \end{aligned} \tag{3.19}$$

with $\boldsymbol{b}^k := \boldsymbol{b}(\cdot, t^k)$ and $\ell^k := \ell(\cdot, t^k)$, for $k = 1, \dots, n$.

Proof. Taking $\boldsymbol{v}_h = \boldsymbol{u}_h^n - \boldsymbol{u}_h^{n-1}$ in (3.17a) gives

$$a_1^h(\boldsymbol{u}_h^n, \boldsymbol{u}_h^n - \boldsymbol{u}_h^{n-1}) + b_1(\boldsymbol{u}_h^n - \boldsymbol{u}_h^{n-1}, \psi_h^n) = F^{h,n}(\boldsymbol{u}_h^n - \boldsymbol{u}_h^{n-1}). \tag{3.20}$$

A use of (3.7c) for the time step n, $n-1$ and setting $\phi_h = -\psi_h^n$, (3.17c) becomes

$$-b_1(\boldsymbol{u}_h^n - \boldsymbol{u}_h^{n-1}, \psi_h^n) - b_2(p_h^n - p_h^{n-1}, \psi_h^n) + a_3(\psi_h^n - \psi_h^{n-1}, \psi_h^n) = 0. \tag{3.21}$$

Adding (3.21) and (3.20) readily gives

$$a_1^h(\boldsymbol{u}_h^n, \boldsymbol{u}_h^n - \boldsymbol{u}_h^{n-1}) + a_3(\psi_h^n - \psi_h^{n-1}, \psi_h^n) - b_2(p_h^n - p_h^{n-1}, \psi_h^n) = F^{h,n}(\boldsymbol{u}_h^n - \boldsymbol{u}_h^{n-1}), \tag{3.22}$$

and choosing $q_h = p_h^n$ in (3.17b) implies the relation

$$\tilde{a}_2^h(p_h^n - p_h^{n-1}, p_h^n) + \Delta t\, a_2^h(p_h^n, p_h^n) - b_2(p_h^n, \psi_h^n - \psi_h^{n-1}) = \Delta t\, G^{h,n}(p_h^n). \tag{3.23}$$

Next we proceed to adding (3.22) and (3.23), to get

$$\begin{aligned} &a_1^h(\boldsymbol{u}_h^n, \boldsymbol{u}_h^n - \boldsymbol{u}_h^{n-1}) + \Delta t\, a_2^h(p_h^n, p_h^n) + a_3(\psi_h^n - \psi_h^{n-1}, \psi_h^n) \\ &\qquad + \tilde{a}_2^h(p_h^n - p_h^{n-1}, p_h^n) - b_2(p_h^n - p_h^{n-1}, \psi_h^n) - b_2(p_h^n, \psi_h^n - \psi_h^{n-1}) \\ &= F^{h,n}(\boldsymbol{u}_h^n - \boldsymbol{u}_h^{n-1}) + \Delta t\, G^{h,n}(p_h^n). \end{aligned}$$

Repeating a similar argument as the one used to obtain (3.11), together with the inequality

$$(f_h^n - f_h^{n-1}, f_h^n) \geq \frac{1}{2}\big(\|f_h^n\|_0^2 - \|f_h^{n-1}\|_0^2\big), \tag{3.24}$$

for any discrete function f_h^j, $j = 1, \ldots, n$, we arrive at

$$\begin{aligned} &\frac{\mu}{2}(\|\boldsymbol{\varepsilon}(\boldsymbol{u}_h^n)\|_0^2 - \|\boldsymbol{\varepsilon}(\boldsymbol{u}_h^{n-1})\|_0^2) + (\Delta t)\frac{\kappa_{\min}}{\eta}\|\nabla p_h^n\|_0^2 + \frac{1}{2}\sum_K c_0(\|\Pi_K^0 p_h^n\|_{0,K}^2 - \|\Pi_K^0 p_h^{n-1}\|_{0,K}^2) \\ &\quad + \frac{1}{2}\Big(c_0 + \frac{\alpha^2}{\lambda}\Big)\sum_K(\|(I - \Pi_K^0)p_h^n\|_{0,K}^2 - \|(I - \Pi_K^0)p_h^{n-1}\|_{0,K}^2) \\ &\quad + \frac{1}{2\lambda}\sum_K(\|\alpha\Pi_K^0 p_h^n - \psi_h^n\|_{0,K}^2 - \|\alpha\Pi_K^0 p_h^{n-1} - \psi_h^{n-1}\|_{0,K}^2) \\ &\lesssim (\Delta t)(\rho(\boldsymbol{b}_h^n, \delta_t \boldsymbol{u}_h^n)_{0,\Omega} + (\ell_h^n, p_h^n)_{0,\Omega}), \end{aligned}$$

where we have denoted $\delta_t f_h(t_n) := \frac{f_h(t_n) - f_h(t_{n-1})}{\Delta t}$ for any time-space discrete function f_h. Summing over n we obtain

$$\begin{aligned} &\frac{\mu}{2}(\|\boldsymbol{\varepsilon}(\boldsymbol{u}_h^n)\|_0^2 - \|\boldsymbol{\varepsilon}(\boldsymbol{u}_h^0)\|_0^2) + (\Delta t)\frac{\kappa_{\min}}{\eta}\sum_{j=1}^n\|\nabla p_h^j\|_0^2 + \frac{1}{2}\sum_K c_0(\|\Pi_K^0 p_h^n\|_{0,K}^2 - \|\Pi_K^0 p_h^0\|_{0,K}^2) \\ &\quad + \frac{1}{2}\Big(c_0 + \frac{\alpha^2}{\lambda}\Big)\sum_K(\|(I - \Pi_K^0)p_h^n\|_{0,K}^2 - \|(I - \Pi_K^0)p_h^0\|_{0,K}^2) \\ &\quad + \frac{1}{2\lambda}\sum_K(\|\alpha\Pi_K^0 p_h^n - \psi_h^n\|_{0,K}^2 - \|\alpha\Pi_K^0 p_h^0 - \psi_h^0\|_{0,K}^2) \\ &\lesssim \underbrace{\rho(\Delta t)\sum_{j=1}^n(\boldsymbol{b}_h^j, \delta_t \boldsymbol{u}_h^j)_{0,\Omega}}_{=:J_1} + \underbrace{(\Delta t)\sum_{j=1}^n(\ell_h^j, p_h^j)_{0,\Omega}}_{=:J_2}. \end{aligned}$$

Using the equality

$$\sum_{j=1}^n(f_h^j - f_h^{j-1}, g_h^j) = (f_h^n, g_h^n) - (f_h^0, g_h^0) - \sum_{j=1}^n(f_h^{j-1}, g_h^j - g_h^{j-1}), \tag{3.25}$$

for any discrete functions f_h^j, g_h^j, $j = 1, \ldots, n$, along with Taylor expansion, Cauchy–Schwarz, Korn's inequality and generalised Young's inequality gives

$$
\begin{aligned}
J_1 &= \rho\Big((\boldsymbol{b}_h^n, \boldsymbol{u}_h^n)_{0,\Omega} - (\boldsymbol{b}_h^0, \boldsymbol{u}_h^0)_{0,\Omega} - \sum_{j=1}^{n}(\boldsymbol{b}_h^j - \boldsymbol{b}_h^{j-1}, \boldsymbol{u}_h^{j-1})_{0,\Omega}\Big) \\
&= \rho\Big((\boldsymbol{b}_h^n, \boldsymbol{u}_h^n)_{0,\Omega} - (\boldsymbol{b}_h^0, \boldsymbol{u}_h^0)_{0,\Omega} - \Delta t\sum_{j=1}^{n}(\partial_t \boldsymbol{b}_h^j, \boldsymbol{u}_h^{j-1})_{0,\Omega} \\
&\quad + \sum_{j=1}^{n}\Big(\int_{t_{j-1}}^{t_j}(s - t_{j-1})\partial_{tt}\boldsymbol{b}_h(s)\,\mathrm{d}s, \boldsymbol{u}_h^{j-1}\Big)_{0,\Omega}\Big) \\
&\leq \mu\|\boldsymbol{\varepsilon}(\boldsymbol{u}_h^0)\|_0^2 + \frac{\mu}{4}\|\boldsymbol{\varepsilon}(\boldsymbol{u}_h^n)\|_0^2 + C(\rho,\mu)\max_{0\leq j\leq n}\|\boldsymbol{b}^j\|_0^2 \\
&\quad + C(\rho)(\Delta t)\sum_{j=1}^{n}\Big(\|\partial_t \boldsymbol{b}^j\|_0 + \Big((\Delta t)\int_{t_{j-1}}^{t_j}\|\partial_{tt}\boldsymbol{b}(s)\|_0^2\,\mathrm{d}s\Big)^{1/2}\Big)\|\boldsymbol{\varepsilon}(\boldsymbol{u}_h^{j-1})\|_0.
\end{aligned}
$$

Another application of Young's inequality yields

$$
J_2 \leq C_2(\eta, \kappa_{\min})(\Delta t)\sum_{j=1}^{n}\|\ell^j\|_0^2 + (\Delta t)\frac{\kappa_{\min}}{2\eta}\sum_{j=1}^{n}\|p_h^j\|_0^2.
$$

The bounds obtained for J_1, J_2 , Π_K^0 and use of Lemma 3.2 imply

$$
\begin{aligned}
&\mu\|\boldsymbol{\varepsilon}(\boldsymbol{u}_h^n)\|_0^2 + c_0\|p_h^n\|_0^2 + (\Delta t)\frac{\kappa_{\min}}{\eta}\sum_{j=1}^{n}\|\nabla p_h^j\|_0^2 \qquad (3.26)\\
&+ \Big(\frac{\alpha^2}{\lambda}\Big)\sum_K\|(I - \Pi_K^0)p_h^n\|_{0,K}^2 + \frac{1}{\lambda}\sum_K\|\alpha\Pi_K^0 p_h^n - \psi_h^n\|_{0,K}^2 \\
&\quad \lesssim \mu\|\boldsymbol{\varepsilon}(\boldsymbol{u}_h^0)\|_0^2 + \Big(c_0 + \frac{\alpha^2}{\lambda}\Big)\|p_h^0\|_0^2 + \frac{1}{\lambda}\|\psi_h^0\|_0^2 + \max_{0\leq j\leq n}\|\boldsymbol{b}^j\|_0^2 + (\Delta t)\sum_{j=1}^{n}\|\ell^j\|_0^2 \qquad (3.27)\\
&\quad + (\Delta t)^2\Big(\sum_{j=1}^{n}\|\partial_t\boldsymbol{b}^j\|_0^2 + (\Delta t)\int_0^T\|\partial_{tt}\boldsymbol{b}(s)\|_0^2\,\mathrm{d}s\Big).
\end{aligned}
$$

An application of (3.6) together with (3.17a) yields

$$
\|\psi_h^n\|_0 \leq C(\|\boldsymbol{b}^n\|_0 + \|\boldsymbol{\varepsilon}(\boldsymbol{u}_h^n)\|_0). \tag{3.28}
$$

Finally, the bound (3.26) together with (3.28) concludes (3.19). □

It is worth pointing out that the proof is particularly delicate since the stabilisation term requires a careful treatment in order to guarantee that the bounds remain independent of the stability constants of the bilinear form $\tilde{a}_2(\cdot,\cdot)$.

Corollary 3.2 (Solvability of the fully discrete problem) *The problem (3.17) has a unique solution in* $\boldsymbol{V}_h \times Q_h \times Z_h$.

Proof. It is sufficient to show that the homogeneous linear system corresponding to (3.17) has only a trivial solution, since $\boldsymbol{V}_h, Q_h$ and Z_h are finite dimensional spaces, and this can easily be shown by proceeding analogously to the proof of Corollary 3.1. □

4 A priori error estimates

For the sake of error analysis, we require additional regularity: In particular, for any $t > 0$, we consider that the displacement is $\boldsymbol{u}(t) \in [H^2(\Omega)]^2$, the fluid pressure $p(t) \in H^2(\Omega)$, and the total pressure $\psi(t) \in H^1(\Omega)$. Furthermore, our subsequent analysis also requires the following regularity in time: $\partial_t \boldsymbol{u} \in \boldsymbol{L}^2(0,T;[H^2(\Omega)]^2)$, $\partial_t p \in L^2(0,T;H^2(\Omega))$, $\partial_t \psi \in L^2(0,T;H^1(\Omega))$, $\partial_{tt}\boldsymbol{u} \in \boldsymbol{L}^2(0,T;[L^2(\Omega)]^2)$ and $\partial_{tt}p, \partial_{tt}\psi \in L^2(0,T;L^2(\Omega))$.

We start by recalling an estimate for the interpolant $\boldsymbol{u}_I \in \boldsymbol{V}_h$ of $\boldsymbol{u}$ and $p_I \in Q_h$ of p (see [5,21,22,42]).

Lemma 4.1 *There exist interpolants $\boldsymbol{u}_I \in \boldsymbol{V}_h$ and $p_I \in Q_h$ of $\boldsymbol{u}$ and p, respectively, such that*

$$\|\boldsymbol{u}-\boldsymbol{u}_I\|_0 + h|\boldsymbol{u}-\boldsymbol{u}_I|_1 \le Ch^2|\boldsymbol{u}|_2, \quad \|p-p_I\|_0 + h|p-p_I|_1 \le Ch^2|p|_2.$$

We now introduce the poroelastic projection operator: given $(\boldsymbol{u},p,\psi) \in \boldsymbol{V}\times Q\times Z$, find $I^h := (I^h_{\boldsymbol{u}}\boldsymbol{u}, I^h_p p, I^h_\psi \psi) \in \boldsymbol{V}_h \times Q_h \times Z_h$ such that

$$a_1^h(I^h_{\boldsymbol{u}}\boldsymbol{u},\boldsymbol{v}_h) + b_1(\boldsymbol{v}_h, I^h_\psi\psi) = a_1(\boldsymbol{u},\boldsymbol{v}_h) + b_1(\boldsymbol{v}_h,\psi) \quad \text{for all } \boldsymbol{v}_h \in \boldsymbol{V}_h, \tag{4.1a}$$

$$b_1(I^h_{\boldsymbol{u}}\boldsymbol{u},\phi_h) = b_1(\boldsymbol{u},\phi_h) \quad \text{for all } \phi_h \in Z_h, \tag{4.1b}$$

$$a_2^h(I^h_p p, q_h) = a_2(p,q_h) \quad \text{for all } q_h \in Q_h, \tag{4.1c}$$

and we remark that I^h is defined by the combination of the saddle-point problem (4.1a), (4.1b) and the elliptic problem (4.1c); and hence, it is well-defined.

Theorem 4.1 (Estimates for the poroelastic projection) *Let $(\boldsymbol{u},p,\psi)$ and $(I^h_{\boldsymbol{u}}\boldsymbol{u}, I^h_p p, I^h_\psi\psi)$ be the unique solutions of (3.7a)–(3.7c) and (4.1a), (4.1b), respectively. Then the following estimates hold:*

$$\|\boldsymbol{u}-I^h_{\boldsymbol{u}}\boldsymbol{u}\|_1 + \|\psi - I^h_\psi\psi\|_0 \le Ch(|\boldsymbol{u}|_2 + |\psi|_1), \tag{4.2a}$$

$$\|p - I^h_p p\|_0 + h\|p - I^h_p p\|_1 \le Ch^2|p|_2. \tag{4.2b}$$

Proof. The estimates available for discretisations of Stokes [5] and elliptic problems [10] conclude the statement. □

Remark 4.1 Note that repeating the same arguments exploited in this and in the subsequent sections, it is possible to derive error estimates of order h^s. It suffices to assume that $\boldsymbol{u}(t) \in [H^{1+s}(\Omega)]^2$, $p(t) \in H^{1+s}(\Omega)$, and $\psi(t) \in H^s(\Omega)$, for $0 < s \le 1$.

Theorem 4.2 (Semi-discrete energy error estimates) *Let the triplets $(\boldsymbol{u}(t),p(t),\psi(t)) \in \boldsymbol{V}\times Q\times Z$ and $(\boldsymbol{u}_h(t),p_h(t),\psi_h(t)) \in \boldsymbol{V}_h\times Q_h\times Z_h$ be the unique solutions to problems (2.3a)–(2.3c) and (3.7a)–(3.7c), respectively. Then, the following bounds hold, with constants $C>0$ independent of h, λ and c_0,*

$$\mu\|\boldsymbol{\varepsilon}((\boldsymbol{u}-\boldsymbol{u}_h)(t))\|_0^2 + \|(\psi-\psi_h)(t)\|_0^2 + \frac{\kappa_{\min}}{\eta}\int_0^t \|\nabla(p-p_h)(s)\|_0^2\,\mathrm{d}s \;\le\; C\,h^2.$$

Proof. Invoking the Scott-Dupont Theory (see [19]) for the polynomial approximation: there exists a constant $C>0$ such that for every s with $0 \le s \le 1$ and for every $u \in H^{1+s}(K)$, there exists $u_\pi \in \mathbb{P}_k(K)$, $k=0,1$, such that

$$\|u-u_\pi\|_{0,K} + h_K|u-u_\pi|_{1,K} \le Ch_K^{1+s}|u|_{1+s,K} \quad \text{for all } K \in \mathcal{T}_h. \tag{4.3}$$

We can then write the displacement and total pressure error in terms of the poroelastic projector as follows

$$(\boldsymbol{u}-\boldsymbol{u}_h)(t) = (\boldsymbol{u}-I^h_{\boldsymbol{u}}\boldsymbol{u})(t) + (I^h_{\boldsymbol{u}}\boldsymbol{u}-\boldsymbol{u}_h)(t) := e^I_{\boldsymbol{u}}(t) + e^A_{\boldsymbol{u}}(t),$$

$$(\psi - \psi_h)(t) = (\psi - I_\psi^h \psi)(t) + (I_\psi^h \psi - \psi_h)(t) := e_\psi^I(t) + e_\psi^A(t).$$

Then, a combination of equations (4.1a), (3.7a) and (2.3a) gives

$$a_1^h(e_{\boldsymbol{u}}^A, \boldsymbol{v}_h) + b_1(\boldsymbol{v}_h, e_\psi^A) = (a_1(\boldsymbol{u}, \boldsymbol{v}_h) - a_1^h(\boldsymbol{u}_h, \boldsymbol{v}_h)) + b_1(\boldsymbol{v}_h, \psi - \psi_h) = (F - F^h)(\boldsymbol{v}_h),$$

and taking as test function $\boldsymbol{v}_h = \partial_t e_{\boldsymbol{u}}^A$, we can write the relation

$$a_1^h(e_{\boldsymbol{u}}^A, \partial_t e_{\boldsymbol{u}}^A) + b_1(\partial_t e_{\boldsymbol{u}}^A, e_\psi^A) = (F - F^h)(\partial_t e_{\boldsymbol{u}}^A). \tag{4.4}$$

Now, we write the pressure error in terms of the poroelastic projector as follows

$$(p - p_h)(t) = (p - I_p^h p)(t) + (I_p^h p - p_h)(t) := e_p^I(t) + e_p^A(t).$$

Using (4.1c), (3.7b) and (2.3b), we obtain

$$\begin{aligned}
&\tilde{a}_2^h(\partial_t e_p^A, q_h) + a_2^h(e_p^A, q_h) - b_2(q_h, \partial_t e_\psi^A) \\
&= \tilde{a}_2^h(\partial_t I_p^h p, q_h) + a_2(p, q_h) - b_2(q_h, \partial_t I_\psi^h \psi) - G^h(q_h) \\
&= (\tilde{a}_2^h(\partial_t I_p^h p, q_h) - \tilde{a}_2(\partial_t p, q_h)) + b_2(q_h, \partial_t e_\psi^I) + (G - G^h)(q_h).
\end{aligned}$$

We can take $q_h = e_p^A$, which leads to

$$\begin{aligned}
&\tilde{a}_2^h(\partial_t e_p^A, e_p^A) + a_2^h(e_p^A, e_p^A) - b_2(e_p^A, \partial_t e_\psi^A) \\
&= (\tilde{a}_2^h(\partial_t I_p^h p, e_p^A) - \tilde{a}_2(\partial_t p, e_p^A)) + b_2(e_p^A, \partial_t e_\psi^I) + (G - G^h)(e_p^A).
\end{aligned} \tag{4.5}$$

Next we use (4.1b), (3.7c) and (2.3c), and this implies

$$\begin{aligned}
&b_1(e_{\boldsymbol{u}}^A, \phi_h) + b_2(e_p^A, \phi_h) - a_3(e_\psi^A, \phi_h) = b_1(I_{\boldsymbol{u}}^h \boldsymbol{u}, \phi_h) + b_2(I_p^h p, \phi_h) - a_3(I_\psi^h \psi, \phi_h) \\
&= b_1(\boldsymbol{u}, \phi_h) + b_2(I_p^h p, \phi_h) - a_3(I_\psi^h \psi, \phi_h) = -b_2(e_p^I, \phi_h) + a_3(e_\psi^I, \phi_h).
\end{aligned}$$

Differentiating the above equation with respect to time and taking $\phi_h = -e_\psi^A$, we can assert that

$$-b_1(\partial_t e_{\boldsymbol{u}}^A, e_\psi^A) - b_2(\partial_t e_p^A, e_\psi^A) + a_3(\partial_t e_\psi^A, e_\psi^A) = b_2(\partial_t e_p^I, e_\psi^A) - a_3(\partial_t e_\psi^I, e_\psi^A). \tag{4.6}$$

Then we simply add (4.4), (4.5) and (4.6), to obtain

$$\begin{aligned}
&a_1^h(e_{\boldsymbol{u}}^A, \partial_t e_{\boldsymbol{u}}^A) + \tilde{a}_2^h(\partial_t e_p^A, e_p^A) + a_2^h(e_p^A, e_p^A) \\
&+ a_3(\partial_t e_\psi^A, e_\psi^A) - b_2(e_p^A, \partial_t e_\psi^A) - b_2(\partial_t e_p^A, e_\psi^A) \\
&= (F - F^h)(\partial_t e_{\boldsymbol{u}}^A) + (\tilde{a}_2^h(\partial_t I_p^h p, e_p^A) - \tilde{a}_2(\partial_t p, e_p^A)) \\
&\quad + b_2(e_p^A, \partial_t e_\psi^I) + (G - G^h)(e_p^A) + b_2(\partial_t e_p^I, e_\psi^A) - a_3(\partial_t e_\psi^I, e_\psi^A).
\end{aligned} \tag{4.7}$$

Regarding the left-hand side of (4.7), repeating arguments to obtain alike to (3.11). That is,

$$\begin{aligned}
&a_1^h(e_{\boldsymbol{u}}^A, \partial_t e_{\boldsymbol{u}}^A) + \tilde{a}_2^h(\partial_t e_p^A, e_p^A) + a_2^h(e_p^A, e_p^A) + a_3(\partial_t e_\psi^A, e_\psi^A) - b_2(e_p^A, \partial_t e_\psi^A) - b_2(\partial_t e_p^A, e_\psi^A) \\
&\geq \frac{1}{2}\frac{\mathrm{d}}{\mathrm{d}t} a_1^h(e_{\boldsymbol{u}}^A, e_{\boldsymbol{u}}^A) + \frac{c_0}{2}\frac{\mathrm{d}}{\mathrm{d}t}\|e_p^A\|_0^2 + a_2^h(e_p^A, e_p^A) \\
&\qquad + \frac{1}{\lambda}\sum_K \Big(\alpha^2 \big(\partial_t(\Pi_K^0 e_p^A), \Pi_K^0 e_p^A\big)_{0,K} + \alpha^2 S_0^K\big((I - \Pi_K^0)\partial_t e_p^A, (I - \Pi_K^0) e_p^A\big) \\
&\qquad + (\partial_t e_\psi^A, e_\psi^A)_{0,K} - \alpha(\Pi_K^0 e_p^A, \partial_t e_\psi^A)_{0,K} - \alpha(\Pi_K^0 \partial_t e_p^A, e_\psi^A)_{0,K}\Big) \\
&\geq C\Big(\mu\frac{\mathrm{d}}{\mathrm{d}t}\|\boldsymbol{\varepsilon}(e_{\boldsymbol{u}}^A)\|_0^2 + c_0\frac{\mathrm{d}}{\mathrm{d}t}\|e_p^A\|_0^2 + \frac{2\kappa_{\min}}{\eta}\|\nabla e_p^A\|_0^2 \\
&\qquad + \frac{1}{\lambda}\sum_K\Big(\alpha^2\frac{\mathrm{d}}{\mathrm{d}t}\|(I - \Pi_K^0)e_p^A\|_{0,K}^2 + \frac{\mathrm{d}}{\mathrm{d}t}\|\alpha\Pi_K^0 e_p^A - e_\psi^A\|_{0,K}^2\Big)\Big).
\end{aligned}$$

Then integrating equation (4.7) in time and consistency of the bilinear term $\tilde{a}_2(\cdot,\cdot)$ implies the bound

$$
\begin{aligned}
&\mu\|\boldsymbol{\varepsilon}(e_{\boldsymbol{u}}^A(t))\|_0^2 + c_0\|e_p^A(t)\|_0^2 + \frac{\kappa_{\min}}{\eta}\int_0^t \|\nabla e_p^A(s)\|_0^2\,\mathrm{d}s \\
&+ \frac{1}{\lambda}\sum_K\Big(\alpha^2\|(I-\Pi_K^0)e_p^A(t)\|_{0,K}^2 + \|(\alpha\Pi_K^0 e_p^A - e_\psi^A)(t)\|_{0,K}^2\Big) \\
&\lesssim \mu\|\boldsymbol{\varepsilon}(e_{\boldsymbol{u}}^A(0))\|_0^2 + c_0\|e_p^A(0)\|_0^2 \\
&\quad + \frac{1}{\lambda}\sum_K\Big(\alpha^2\|(I-\Pi_K^0)e_p^A(0)\|_{0,K}^2 + \|(\alpha\Pi_K^0 e_p^A - e_\psi^A)(0)\|_{0,K}^2\Big) \\
&\quad + \underbrace{\rho\int_0^t \big((\boldsymbol{b}-\boldsymbol{b}^h)(s), \partial_t e_{\boldsymbol{u}}^A(s)\big)_{0,\Omega}\,\mathrm{d}s}_{=:D_1} + \underbrace{\int_0^t \big((\ell-\ell^h)(s), e_p^A(s)\big)_{0,\Omega}\,\mathrm{d}s}_{=:D_2} \\
&\quad + \underbrace{\int_0^t \sum_K\Big(\tilde{a}_2^{h,K}\big(\partial_t(I_p^h p - p_\pi)(s), e_p^A(s)\big) - \tilde{a}_2^K\big(\partial_t(p-p_\pi)(s), e_p^A(s)\big)\Big)\,\mathrm{d}s}_{=:D_3} \\
&\quad + \underbrace{\int_0^t \Big(b_2\big(e_p^A(s), \partial_t e_\psi^I(s)\big) + b_2\big(\partial_t e_p^I(s), e_\psi^A(s)\big) - a_3\big(\partial_t e_\psi^I(s), e_\psi^A(s)\big)\Big)\,\mathrm{d}s}_{=:D_4}\,.
\end{aligned}
$$

Then we can integrate by parts (also in time), use Cauchy-Schwarz inequality and Young's inequality to arrive at

$$
\begin{aligned}
D_1 &= \rho\bigg(\big((\boldsymbol{b}-\boldsymbol{b}^h)(t), e_{\boldsymbol{u}}^A(t)\big)_{0,\Omega} - \big((\boldsymbol{b}-\boldsymbol{b}^h)(0), e_{\boldsymbol{u}}^A(0)\big)_{0,\Omega} \\
&\qquad - \int_0^t \big(\partial_t(\boldsymbol{b}-\boldsymbol{b}^h)(s), e_{\boldsymbol{u}}^A(s)\big)_{0,\Omega}\,\mathrm{d}s\bigg) \\
&\le \frac{\mu}{2}\|\boldsymbol{\varepsilon}(e_{\boldsymbol{u}}^A(t))\|_0^2 + C_1(\rho,\mu)h\bigg(h|\boldsymbol{b}(t)|_1^2 + |\boldsymbol{b}(0)|_1\|e_{\boldsymbol{u}}^A(0)\|_0 + \int_0^t |\partial_t\boldsymbol{b}(s)|_1\|e_{\boldsymbol{u}}^A(s)\|_0\,\mathrm{d}s\bigg),
\end{aligned}
$$

where we have used standard error estimate for the L^2-projection $\boldsymbol{\Pi}_K^{0,0}$ onto piecewise constant functions. Using also Cauchy-Schwarz inequality, standard error estimates for Π_K^0 on the term D_2, Young's and Poincaré inequality readily gives

$$
D_2 \le Ch\int_0^t |\ell(s)|_1\|e_p^A(s)\|_0\;\mathrm{d}s \le C_2h^2\int_0^t |\ell(s)|_1^2\,\mathrm{d}s + \frac{\kappa_{\min}}{6\eta}\int_0^t \|\nabla e_p^A(s)\|_0^2\,\mathrm{d}s.
$$

On the other hand, considering the polynomial approximation p_π (cf. (4.3)) of p , utilising the triangle inequality, Young's and Poincaré inequality yield

$$
\begin{aligned}
D_3 &\le C\Big(c_0 + \frac{\alpha^2}{\lambda}\Big)\int_0^t \sum_K\Big(\|\partial_t(I_p^h p - p_\pi)(s)\|_{0,K} + \|\partial_t(p-p_\pi)(s)\|_{0,K}\Big)\|e_p^A(s)\|_{0,K}\,\mathrm{d}s \\
&\le Ch^2\Big(c_0 + \frac{\alpha^2}{\lambda}\Big)\int_0^t |\partial_t p(s)|_2\|e_p^A(s)\|_0\,\mathrm{d}s \\
&\le C_3h^4\Big(c_0 + \frac{\alpha^2}{\lambda}\Big)^2\int_0^t |\partial_t p(s)|_2^2\,\mathrm{d}s + \frac{\kappa_{\min}}{6\eta}\int_0^t \|\nabla e_p^A(s)\|_0^2\,\mathrm{d}s.
\end{aligned}
$$

Also,

$$
D_4 = \int_0^t \Big(b_2\big(e_p^A(s), \partial_t e_\psi^I(s)\big) + b_2\big(\partial_t e_p^I(s), e_\psi^A(s)\big) - a_3\big(\partial_t e_\psi^I(s), e_\psi^A(s)\big)\Big)\,\mathrm{d}s
$$

$$\leq \frac{1}{\lambda}\int_0^t \Big(\alpha\|e_p^A(s)\|_0\|\partial_t e_\psi^I(s)\|_0 + \big(\alpha\|\partial_t e_p^I(s)\|_0 + \|\partial_t e_\psi^I(s)\|_0\big)\|e_\psi^A(s)\|_0\Big)\,\mathrm{d}s$$
$$\leq \frac{C}{\lambda}h\int_0^t \Big(\alpha\|e_p^A(s)\|_0(|\partial_t\psi(s)|_1 + |\partial_t\boldsymbol{u}(s)|_2)$$
$$+ (\alpha h|\partial_t p(s)|_2 + |\partial_t\psi(s)|_1 + |\partial_t\boldsymbol{u}(s)|_2)\|e_\psi^A(s)\|_0\Big)\,\mathrm{d}s.$$

Using (3.6) and a combination of equations (4.1a), (3.7a) and (2.3a), we get

$$\begin{aligned}\|e_\psi^A(t)\|_0 &\leq \sup_{\boldsymbol{v}_h\in\boldsymbol{V}_h}\frac{b_1(\boldsymbol{v}_h, e_\psi^A(t))}{\|\boldsymbol{v}_h\|_1} \leq C\left(\rho\sum_K\|(\boldsymbol{b}-\boldsymbol{b}^h)(t)\|_{0,K} + \mu\|\boldsymbol{\varepsilon}(e_{\boldsymbol{u}}^A(t))\|_0\right)\\ &\leq C\big(\rho\, h|\boldsymbol{b}(t)|_1 + \mu\|\boldsymbol{\varepsilon}(e_{\boldsymbol{u}}^A(t))\|_0\big).\end{aligned} \tag{4.8}$$

Then the bound of D_4 with the help of Young's and Poincaré inequality becomes

$$D_4 \leq \frac{C_6}{\lambda}h\int_0^t \Big((\alpha h|\partial_t p(s)|_2 + |\partial_t\psi(s)|_1 + |\partial_t\boldsymbol{u}(s)|_2)(\rho h|\boldsymbol{b}(s)|_1 + \mu\|\boldsymbol{\varepsilon}(e_{\boldsymbol{u}}^A(t))\|_0)$$
$$+ \alpha^2\frac{h}{\lambda}(|\partial_t\psi(s)|_1 + |\partial_t\boldsymbol{u}(s)|_2)^2\Big)\,\mathrm{d}s + \frac{\kappa_{\min}}{6\eta}\int_0^t\|\nabla e_p^A(s)\|_0^2\,\mathrm{d}s.$$

Combining the bounds of all $D_i, i = 1,2,3,4$ and proceeding similar fashion as we obtained the bounds in (3.13)(using Lemma 3.1 and (3.9)), eventually allows us to conclude that

$$\mu\|\boldsymbol{\varepsilon}(e_{\boldsymbol{u}}^A(t))\|_0^2 + c_0\|e_p^A(t)\|_0^2 + \frac{\kappa_{\min}}{\eta}\int_0^t\|\nabla e_p^A(s)\|_0^2\,\mathrm{d}s$$
$$\leq \mu\|\boldsymbol{\varepsilon}(e_{\boldsymbol{u}}^A(0))\|_0^2 + \Big(c_0 + \frac{\alpha^2}{\lambda}\Big)\|e_p^A(0)\|_0^2 + \frac{1}{\lambda}\|e_\psi^A(0)\|_0^2$$
$$+ C\,h^2\Big(\sup_{t\in[0,t_{\text{final}}]}|\boldsymbol{b}(t)|_1^2 + \int_0^t\Big(|\boldsymbol{b}(s)|_1^2 + |\partial_t\boldsymbol{b}(s)|_1^2 + |\ell(s)|_1^2$$
$$+ \Big(\frac{1}{\lambda}\Big)^2(|\partial_t\psi(s)|_1^2 + |\partial_t\boldsymbol{u}(s)|_2^2) + \Big(c_0 + \frac{\alpha^2}{\lambda}\Big)^2 h^2|\partial_t p(s)|_2^2\Big)\,\mathrm{d}s\Big).$$

Then choosing $\boldsymbol{u}_h(0) := \boldsymbol{u}_I(0)$, $\psi_h(0) := \Pi^{0,0}\psi(0)$, $p_h(0) := p_I(0)$ and applying the triangle inequality together with (4.8) completes the rest of the proof. □

Following a similar structure to the proof of Theorem 4.2, we can establish error estimates for the fully-discrete problem. Details on the proof are postponed to the Appendix.

Theorem 4.3 (Fully-discrete error estimates) *Let $(\boldsymbol{u}(t), p(t), \psi(t)) \in \boldsymbol{V}\times Q\times Z$ and $(\boldsymbol{u}_h^n, p_h^n, \psi_h^n) \in \boldsymbol{V}_h\times Q_h\times Z_h$ be the unique solutions to problems (2.3a)-(2.3c) and (3.17a)-(3.17c), respectively. Then the following estimates hold for any $n = 1,\dots,N$, with constants C independent of h, Δt, λ and c_0:*

$$\mu\|\boldsymbol{\varepsilon}(\boldsymbol{u}(t_n) - \boldsymbol{u}_h^n)\|_0^2 + \|\psi(t_n) - \psi_h^n\|_0^2 + (\Delta t)\frac{\kappa_{\min}}{\eta}\|\nabla(p(t_n) - p_h^n)\|_0^2 \leq C\,(h^2 + \Delta t^2). \tag{4.9}$$

Remark 4.2 It is well known that an application of Grownwall's lemma implies an exponential dependency of the generic constant (appearing on the right-hand side) on the final time, and the resulting bounds are therefore not very useful for large time intervals. We stress that by following the approach used in [36,37] we are able to establish convergence and stability for the semi- and fully discrete schemes circumventing the use of Gronwall's inequality. A different approach, employed in, e.g., [17] in the context of poroelasticity problems, is to integrate in time the mass conservation equation.

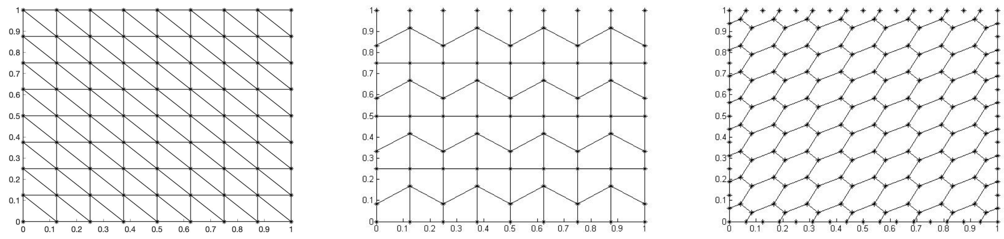

(a) (b) (c)

Fig. 5.1 Samples of triangular (a), distorted quadrilateral (b), and hexagonal (c) meshes employed for the numerical tests in this section.

5 Numerical results

In this section conduct numerical tests to computationally reconfirm the convergence rates of the proposed virtual element scheme and present one test of applicative interest in poromechanics. All numerical results are produced by an in-house MATLAB code, using sparse factorisation as linear solver.

5.1 Verification of spatial convergence

First we consider a steady version of the poroelasticity equations. An exact solution of the problem on the square domain $(0,1)^2$ is given by the smooth functions

$$\boldsymbol{u}(x,y) = \begin{pmatrix} -\cos(2\pi x)\ \sin(2\pi y) + \sin(2\pi y) + \sin^2(\pi x)\sin^2(\pi y) \\ \sin(2\pi x)\cos(2\pi y) - \sin(2\pi x) \end{pmatrix},$$
$$p(x,y) = \sin^2(\pi x)\sin^2(\pi y), \quad \psi(x,y) = \alpha p - \lambda \operatorname{div} \boldsymbol{u}.$$

The body load $\boldsymbol{f}$ and the fluid source ℓ are computed by evaluating these closed-form solutions and the problem is completely characterised after specifying the model constants

$$\nu = 0.3, \quad E_c = 100, \quad \kappa = 1, \quad \alpha = 1, \quad c_0 = 1, \quad \eta = 0.1, \quad \lambda = \frac{E_c \nu}{(1+\nu)(1-2\nu)}, \quad \mu = \frac{E_c}{(2+2\nu)}.$$

On a sequence of successively refined grids (we have employed for this particular case, uniform triangular meshes as depicted in Figure 5.1(a)) we compute errors and convergence rates according to the meshsize and tabulating also the total number of degrees of freedom (Ndof). The experimental error decay (with respect to mesh refinement) is measured using individual relative norms defined as follows:

$$e_1(\boldsymbol{u}) := \frac{\left(\sum_{K\in\mathcal{T}_h} |\boldsymbol{u} - \boldsymbol{\Pi}^{\boldsymbol{\varepsilon}}_K \boldsymbol{u}_h|^2_{1,K}\right)^{1/2}}{|\boldsymbol{u}|_{1,\Omega}}, \quad e_0(\boldsymbol{u}) := \frac{\left(\sum_{K\in\mathcal{T}_h} \|\boldsymbol{u} - \boldsymbol{\Pi}^{\boldsymbol{\varepsilon}}_K \boldsymbol{u}_h\|^2_{0,K}\right)^{1/2}}{\|\boldsymbol{u}\|_{0,\Omega}},$$
$$e_1(p) := \frac{\left(\sum_{K\in\mathcal{T}_h} |p - \Pi^{\nabla}_K p_h|^2_{1,K}\right)^{1/2}}{|p|_{1,\Omega}}, \quad e_0(p) := \frac{\left(\sum_{K\in\mathcal{T}_h} \|p - \Pi^{\nabla}_K p_h\|^2_{0,K}\right)^{1/2}}{\|p\|_{0,\Omega}},$$
$$e_0(\psi) := \frac{\left(\sum_{K\in\mathcal{T}_h} \|\psi - \psi_h\|^2_{0,K}\right)^{1/2}}{\|\psi\|_{0,\Omega}},$$

and Table 5.1 shows the convergence history, exhibiting optimal error decay.

Ndof	h	$e_1(\boldsymbol{u})$	r	$e_0(\boldsymbol{u})$	r	$e_0(\psi)$	r	$e_1(p)$	r	$e_0(p)$	r
179	0.25	0.477968	-	0.271687	-	0.508386	-	0.444463	-	0.142539	-
819	0.125	0.204990	1.22	0.055766	2.28	0.198845	1.35	0.195632	1.18	0.029745	2.26
3419	0.0625	0.097838	1.07	0.013083	2.09	0.091837	1.11	0.097854	1.00	0.007526	1.98
13819	0.03125	0.049954	0.97	0.003322	1.98	0.043829	1.07	0.024456	1.02	0.001842	2.03
56067	0.015625	0.024756	1.01	$8.2 \cdot 10^{-4}$	2.02	0.021704	1.01	0.024456	0.98	$4.7 \cdot 10^{-4}$	1.96

Table 5.1 Verification of space convergence for the method with $k = 1$. Errors and convergence rates r for solid displacement, total pressure and fluid pressure.

Δt	$E_0(\boldsymbol{u})$	r	$E_0(p)$	r	$E_0(\psi)$	r
0.5	0.002897	–	0.462768	–	0.398059	–
0.25	0.001362	1.09	0.218179	1.08	0.187834	1.08
0.125	$6.5173 \cdot 10^{-4}$	1.06	0.104546	1.06	0.090044	1.06
0.0625	$3.1756 \cdot 10^{-4}$	1.04	0.050955	1.04	0.043910	1.04
0.03125	$1.5664 \cdot 10^{-4}$	1.02	0.025123	1.02	0.021683	1.02
0.015625	$7.7950 \cdot 10^{-5}$	1.01	0.012469	1.01	0.010826	1.00

Table 5.2 Convergence of the time discretisation for solid displacement, fluid pressure, and total pressure, using successive partitions of the time interval and a fixed hexagonal mesh.

5.2 Convergence with respect to the time advancing scheme

Regarding the convergence of the time discretisation, we fix a relatively fine hexagonal mesh and construct successively refined partitions of the time interval $(0, 1]$. As in [52], and in order to avoid mixing errors coming from the spatial discretisation, we modify the exact solutions to be

$$\boldsymbol{u}(x, y, t) = 100 \sin(t) \begin{pmatrix} \frac{x}{\lambda} + y, \\ x + \frac{y}{\lambda} \end{pmatrix}, \quad p(x, y, t) = \sin(t)(x + y), \quad \psi(x, y, t) = \alpha p - \lambda \operatorname{div} \boldsymbol{u},$$

and we use them to compute loads, sources, initial data, boundary values, and boundary fluxes. The model parameters assume the values

$$\kappa = 0.1, \quad \alpha = 1, \quad c_0 = 0, \quad \eta = 1, \quad \lambda = 1 \times 10^3 \quad \mu = 1. \tag{5.1}$$

The boundary definition is $\Gamma = [\{0\} \times (0, 1)] \cup [(0, 1) \times \{0\}]$ (bottom and left edges) and $\Sigma = \partial\Omega \setminus \Gamma$.

We recall that cumulative errors up to t_{final} associated with solid displacement, fluid pressure, and a generic pressure v (representing either fluid or total pressure), are defined as

$$\begin{aligned} E_0(\boldsymbol{u}) &= \left(\Delta t \sum_{n=1}^{N} \left(\sum_{K \in \mathcal{T}_h} \|\boldsymbol{u}(t_n) - \boldsymbol{\Pi}_K^{\boldsymbol{\varepsilon}} \boldsymbol{u}_h^n\|_{0,K}^2 \right) \right)^{1/2}, \\ E_0(v) &= \left(\Delta t \sum_{n=1}^{N} \left(\sum_{K \in \mathcal{T}_h} \|v(t_n) - \Pi_K^{\nabla} v_h^n\|_{0,K}^2 \right) \right)^{1/2}, \end{aligned} \tag{5.2}$$

respectively. From Table 5.2 we can readily observe that these errors decay with a rate of $O(\Delta t)$.

5.3 Verification of simultaneous space-time convergence for poroelasticity

Now we consider exact solid displacement and fluid pressure solving problem (2.1) on the square domain $\Omega = (0, 1)^2$ and on the time interval $(0, 1]$, given as

$$\boldsymbol{u}(x, y, t) = \begin{pmatrix} -\exp(-t)\sin(2\pi y)(1 - \cos(2\pi x)) + \frac{\exp(-t)}{\mu+\lambda} \sin(\pi x)\sin(\pi y) \\ \exp(-t)\sin(2\pi x)(1 - \cos(2\pi y)) + \frac{\exp(-t)}{\mu+\lambda} \sin(\pi x)\sin(\pi y) \end{pmatrix},$$

h	Δt	$E_1(\boldsymbol{u})$	r	$E_0(\boldsymbol{u})$	r	$E_1(p)$	r	$E_0(p)$	r	$E_0(\psi)$	r
1/8	1/10	1.741116	-	0.101035	-	0.239518	-	0.009757	-	0.509493	-
1/16	1/20	0.892377	0.96	0.026166	1.95	0.123684	0.95	0.002528	1.95	0.251106	1.02
1/32	1/40	0.451402	0.98	0.006594	1.99	0.062743	0.98	0.000642	1.98	0.125025	1.01
1/64	1/80	0.227050	0.99	0.001650	2.00	0.031584	0.99	0.000161	1.99	0.062399	1.00
1/128	1/160	0.113876	1.00	0.000413	2.00	0.015844	1.00	0.000041	2.00	0.031165	1.00

Table 5.3 Convergence of the numerical method for displacement, fluid pressure, and total pressure, up to the final time $t = 1$, using simultaneous partitions of the time interval and of the spatial domain (using hexagonal meshes).

$$p(x, y, t) = \exp(-t)\sin(\pi x)\sin(\pi y), \quad \psi(x, y, t) = \alpha p - \lambda \operatorname{div} \boldsymbol{u},$$

which satisfies $\operatorname{div} \boldsymbol{u} \to 0$ as $\lambda \to \infty$ (see similar tests in [24, 54]). The load functions, boundary values, and initial data can be obtained from these closed-form solutions, and alternatively to the dilation modulus and permeability specified in (5.1), we here choose larger values $\lambda = 1 \times 10^4$, and $\kappa = 1$.

In addition to the errors in (5.2), for displacement and for fluid pressure we will also compute

$$E_1(\boldsymbol{u}) = \left(\Delta t \sum_{n=1}^{N} \left(\sum_{K \in \mathcal{T}_h} |\boldsymbol{u}(t_n) - \boldsymbol{\Pi}_K^{\boldsymbol{\varepsilon}} \boldsymbol{u}_h^n|_{1,K}^2 \right) \right)^{1/2},$$

$$E_1(p) = \left(\Delta t \sum_{n=1}^{N} \left(\sum_{K \in \mathcal{T}_h} |p(t_n) - \Pi_K^{\nabla} p_h^n|_{1,K}^2 \right) \right)^{1/2}.$$

We consider here pure Dirichlet boundary conditions for both displacement and fluid pressure. A backward Euler time discretisation is used, and in this case we are using successive refinements of the hexagonal partition of the domain as shown in Figure 5.1(c), simultaneously with a successive refinement of the time step. The cumulative errors are again computed until the final time $t = 1$, and the results are collected in Table 5.3. They show once more optimal convergence rates for the scheme in its lowest-order form.

Note from this and the previous test, that a zero constrained specific storage coefficient does not hinder the convergence properties.

5.4 Gradual compression of a poroelastic block

Finally we carry out a test involving the compression of a block occupying the region $\Omega = (0, 1)^2$ by applying a sinusoidal-in-time traction on a small region on the top of the box (see a similar test in [45]). The model parameters in this case are

$$\nu = 0.49995, \quad E_c = 3 \times 10^4, \quad \kappa = 1 \times 10^{-4}, \quad \alpha = 1, \quad c_0 = 1 \times 10^{-3},$$
$$\eta = 1, \quad \lambda = \frac{E_c \nu}{(1+\nu)(1-2\nu)}, \quad \mu = \frac{E_c}{(2+2\nu)}.$$

For this test we have employed a mesh conformed by distorted quadrilaterals exemplified in Figure 5.1(b). The boundary conditions are of homogeneous Dirichlet type for fluid pressure on the whole boundary, and of mixed type for displacement, and the boundary is split as $\partial\Omega := \Gamma_1 \cup \Gamma_2 \cup \Gamma_3$. A traction $\boldsymbol{h}(t) = (0, -1.5 \times 10^4 \sin(\pi t))^T$ is applied on a segment of the top edge of the boundary $\Gamma_1 = (0.25, 0.75) \times \{1\}$, on the remainder of the top edge $\Gamma_2 = [0, 1] \times \{1\} \backslash \Gamma_1$, we impose zero traction, and the body is clamped on the remainder of the boundary $\Gamma_3 = \partial\Omega \backslash (\Gamma_1 \cup \Gamma_2)$. No boundary conditions are prescribed for the total pressure. Initially the system is at rest $\boldsymbol{u}(0) = \boldsymbol{0}$, $\psi(0) = 0$, $p(0) = 0$, and we employ a backward Euler discretisation of the time interval $(0, 0.5]$ with a constant timestep $\Delta t = 0.1$. The numerical results obtained at the final time are depicted in Figure 5.2, where the profiles for fluid and total pressure present no spurious oscillations.

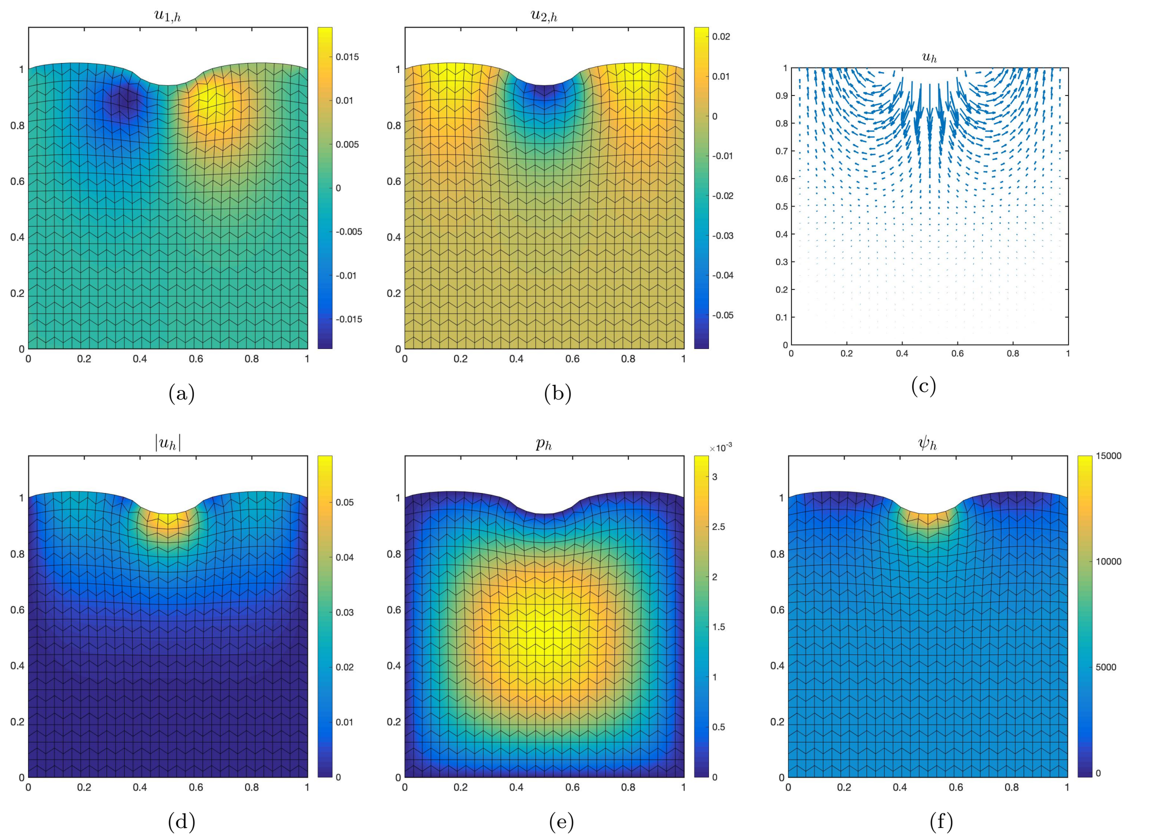

Fig. 5.2 Compression of a poroelastic block after $t = 0.5$ adimensional units. Approximate displacement components (a,b), displacement vectors on the undeformed domain (c), displacement magnitude (d), fluid pressure (e), and total pressure (f), depicted on the deformed domain.

6 Summary and concluding remarks

We have constructed and analysed a new virtual element method for the Biot equations of linear poroelasticity. The finite-dimensional formulation is based on the virtual element spaces introduced in [5], which can be regarded as low-order and stable virtual elements, hence being computationally competitive compared to other existing stable pairs for incompressible flow problems. Both the discrete formulation and its analysis are novel, and they constitute the first fully VEM discretisation for poroelasticity problems. Optimal and Lamé-robust error estimates were established for solid displacement, fluid pressure, and total pressure, in natural norms without weighting. This was achieved with the help of appropriate poroelastic projection operators. Numerical experiments have been performed using different polygonal meshes, and they put into evidence not only computational verification of the convergence of the scheme (where rates of error decay in space and in time are in excellent agreement with the theoretically derived error bounds), but also its performance in simple poromechanical tests.

Natural extensions of this work include the development and analysis of higher-order versions of the virtual discretisations advanced here, the efficient implementation and application to 3D problems, and the coupling with other phenomena such as diffusion of solutes in poroelastic structures [52], interface elasticity-poroelasticity problems [4], multilayer poromechanics [44], or multiple-network consolidation models [37].

Regarding the time discretisation, we have adopted an implicit and monolithic approach, as one enjoys unconditional stability. However, for large scale 3D problems, perhaps a more efficient strategy would consist in using operator splittings, where smaller and better conditioned sub-systems are solved iteratively (see, e.g., the monograph [28] and the references therein). For Biot's consolidation problem and related linear and nonlinear poromechanical systems the literature contains several advanced techniques based on distinct block separations such as undrained split (where the solid motion is resolved for a given fluid pressure) followed by an update, or the converse fixed-stress approach (where the total volumetric stress is considered given during an elliptic pressure solve) [2,15,16,31,32,39,40]. For the three-field formulation written in terms of total pressure, even if this latter splitting would be quite convenient, still the updating of the solid sub-model would involve the solution of a saddle-point system for displacement and total pressure. In any case, if the fixed-point maps defining the operator splitting method are contractive then the stability and convergence of the iterative process would make the resulting approach an appealing method.

Acknowledgements. We thank the valuable comments by two anonymous reviewers, whose suggestions lead to numerous improvements to the manuscript. This work has been partially supported by CONICYT (Chile) through projects FONDECYT 1170473, FONDECYT 1180913, CONICYT/PIA/AFB170001, and CRHIAM, project CONICYT/FONDAP/15130015; by the HPC-Europa3 Transnational Access Grant HPC175QA9K; and by the Department of Science and Technology (DST-SERB), India through MATRICS grant MTR/2019/000519.

References

1. B. Ahmad, A. Alsaedi, F. Brezzi, L.D. Marini, and A. Russo, Equivalent projectors for virtual element methods, *Comput. Math. Appl.* **66** (2013) 376–391.
2. E. Ahmed, J.M. Nordbotten, and F.A. Radu, Adaptive asynchronous time-stepping, stopping criteria, and a posteriori error estimates for fixed-stress iterative schemes for coupled poromechanics problems. *J. Comput. Appl. Math.* **364** (2020) 112312.
3. V. Anaya, M. Bendahmane, D. Mora, and M. Sepúlveda, A virtual element method for a nonlocal FitzHugh-Nagumo model of cardiac electrophysiology, *IMA J. Numer. Anal.* **40**(2) (2020) 1544–1576.
4. V. Anaya, Z. De Wijn, B. Gómez-Vargas, D. Mora, and R. Ruiz Baier, Rotation-based mixed formulations for an elasticity-poroelasticity interface problem, *SIAM J. Sci. Comput.* **42**(1) (2020) B225–B249.
5. P.F. Antonietti, L. Beirão da Veiga, D. Mora, and M. Verani, A stream virtual element formulation of the Stokes problem on polygonal meshes, *SIAM J. Numer. Anal.* **52** (2014) 386–404.
6. P.F. Antonietti, L. Beirão da Veiga, S. Scacchi and M. Verani, A C^1 virtual element method for the Cahn–Hilliard equation with polygonal meshes, *SIAM J. Numer. Anal.* **54** (2016) 36–56.
7. F. Arega and E. Hayter, Coupled consolidation and contaminant transport model for simulating migration of contaminants through the sediment and a cap, *Appl. Math. Model.* **32** (2008) 2413–2428.
8. R. Asadi, B. Ataie-Ashtiani, and C.T. Simmons, Finite volume coupling strategies for the solution of a Biot consolidation model, *Comput. Geotech.* **55** (2014) 494–505.
9. L. Beirão da Veiga, F. Brezzi, A. Cangiani, G. Manzini, L.D. Marini, and A. Russo, Basic principles of virtual element methods, *Math. Models Methods Appl. Sci.* **23** (2013) 199–214.
10. L. Beirão da Veiga, F. Brezzi, L.D. Marini, and A. Russo, Virtual element method for general second-order elliptic problems on polygonal meshes, *Math. Models Methods Appl. Sci.* **26** (2016) 729–750.
11. L. Beirão da Veiga, C. Lovadina, and G. Vacca, Divergence free virtual elements for the Stokes problem on polygonal meshes, *ESAIM: Math. Model. Numer. Anal.* **51** (2017) 509–535.
12. L. Beirão da Veiga and D. Mora, A mimetic discretization of the Reissner-Mindlin plate bending problem, *Numer. Math.* **117** (2011) 425–462.
13. L. Beirão da Veiga, D. Mora, and G. Rivera, Virtual Elements for a shear-deflection formulation of Reissner-Mindlin plates, *Math. Comp.* **88** (2019) 149–178.
14. D. Boffi, M. Botti, and D.A. Di Pietro, A nonconforming high-order method for the Biot problem on general meshes, *SIAM J. Sci. Comput.* **38** (2016) A1508–A1537.
15. M. Borregales, F.A. Radu, K. Kumar, and J.M. Nordbotten, Robust iterative schemes for nonlinear poromechanics, *Comput. Geosci.* **22** (2018) 1021–1038.
16. J.W. Both, M. Borregales, J.M. Nordbotten, K. Kumar, and F.A. Radu, Robust fixed stress splitting for Biot's equations in heterogeneous media, *Appl. Math. Lett.* **68** (2017) 101–108.
17. L. Botti, M. Botti, and Daniele A.Di Pietro, An abstract analysis framework for monolithic discretisations of poroelasticity with application to Hybrid High-Order methods, *Comput. Math. Appl.* (2020) (Available onlne: https://doi.org/10.1016/j.camwa.2020.06.004).
18. S.C. Brenner, Q. Guan and L.-Y Sung, Some estimates for virtual element methods, *Comput. Methods Appl. Math.* **17** (2017) 553–574.
19. S.C. Brenner and L.R. Scott, The mathematical theory of finite element methods, Texts in Applied Mathematics, Springer, New York, (2008) xviii+397pp.
20. E. Cáceres and G.N. Gatica, A mixed virtual element method for the pseudostress-velocity formulation of the Stokes problem, *IMA J. Numer. Anal.* **37** (2017) 296–331.

21. A. Cangiani, E.H. Georgoulis, T. Pryer, and O.J. Sutton, A posteriori error estimates for the virtual element method, *Numer. Math.* **137** (2017) 857–893.
22. A. Cangiani, G. Manzini, and O.J. Sutton, Conforming and nonconforming virtual element methods for elliptic problems, *IMA J. Numer. Anal.* **37** (2017) 1317–1354.
23. J. Coulet, I. Faille, V. Girault, N. Guy, and F. Nataf, A fully coupled scheme using virtual element method and finite volume for poroelasticity, *Comput. Geosci.* **24** (2020) 381–403.
24. G. Fu, A high-order HDG method for the Biot's consolidation model, *Comput. Math. Appl.* **77** (2019) 237–252.
25. F.J. Gaspar, F.J. Lisbona, and P.N. Vabishchevich, Finite difference schemes for poroelastic problems, *Comput. Methods Appl. Math.* **2** (2002) 132–142.
26. V. Girault, G. Pencheva, M.F. Wheeler, and T. Wildey, Domain decomposition for poroelasticity and elasticity with DG jumps and mortars, *Math. Models Methods Appl. Sci.* **21** (2011) 169–213.
27. V. Girault and P.-A. Raviart, Finite Element Methods for Navier-Stokes Equations: Theory and algorithms. Springer Series in Computational Mathematics (1986) (5) x+374pp.
28. H. Holden, K.H. Karlsen, K.A. Lie, and N.H. Risebro, Splitting Methods for Partial Differential Equations with Rough Solutions: Analysis and MATLAB programs. European Mathematical Society (2010).
29. Q. Hong and J. Kraus, Parameter-robust stability of classical three-field formulation of Biot's consolidation model, *Electron. Trans. Numer. Anal.* **48** (2018) 202–226.
30. X. Hu, C. Rodrigo, F.J. Gaspar, and L.T. Zikatanov, A non-conforming finite element method for the Biot's consolidation model in poroelasticity, *J. Comput. Appl. Math.* **310** (2017) 143–154.
31. J. Kim, H.A. Tchelepi, and R. Juanes, Stability, accuracy and efficiency of sequential methods for coupled flow and geomechanics, *SPE J.* **16**(02) (2011) 119084.
32. A.E. Kolesov, P.N. Vabishchevich, and M.V. Vasilyeva, Splitting schemes for poroelasticity and thermoelasticity problems, *Comput. Math. Appl.* **67** (2014) 2185–2198.
33. S. Kumar, R. Oyarzúa, R. Ruiz-Baier, and R. Sandilya, Conservative discontinuous finite volume and mixed schemes for a new four-field formulation in poroelasticity, *ESAIM: Math. Model. Numer. Anal.* **54**(1) (2020) 273–299.
34. J.J. Lee, Analysis and preconditioning of parameter-robust finite element methods for Biot's consolidation model. *Arxiv preprint*, available from arxiv.org/abs/1806.11566.
35. J.J. Lee, K.-A. Mardal, and R. Winther, Parameter-robust discretization and preconditioning of Biot's consolidation model, *SIAM J. Sci. Comput.* **39** (2017) A1–A24.
36. J.J. Lee, Robust three-field finite element methods for Biot's consolidation model in poroelasticity, *Bit Numer Math* **58** (2018) 347—372.
37. J.J. Lee, E. Piersanti, K.-A. Mardal, and M. Rognes, A mixed finite element method for nearly incompressible multiple-network poroelasticity, *SIAM J. Sci. Comput.* **41** (2019) A722–A747.
38. R.T. Mauck, C.T. Hung, and G.A. Ateshian, Modelling of neutral solute transport in a dynamically loaded porous permeable gel: implications for articular cartilage biosynthesis and tissue engineering, *J. Biomech. Engrg.* **125** (2003) 602–614.
39. A. Mikelić, B. Wang, and M.F. Wheeler, Numerical convergence study of iterative coupling for coupled flow and geomechanics, *Comput. Geosci.* **18** (2014) 325–34.
40. A. Mikelić and M.F. Wheeler, Convergence of iterative coupling for coupled flow and geomechanics, *Comput. Geosci.* **17** (2013) 455–461.
41. D. Mora and G. Rivera, A priori and a posteriori error estimates for a virtual element spectral analysis for the elasticity equations, *IMA J. Numer. Anal.* **40**(1) (2020) 322–357.
42. D. Mora, G. Rivera, and R. Rodríguez, A virtual element method for the Steklov eigenvalue problem, *Math. Models Methods Appl. Sci.* **25** (2015) 1421–1445.
43. M.A. Murad, V. Thomée, and A.F.D. Loula, Asymptotic behavior of semi discrete finite-element approximations of Biot's consolidation problem, *SIAM J. Numer. Anal.* **33** (1996) 1065–1083.
44. A. Naumovich, On finite volume discretization of the three-dimensional Biot poroelasticity system in multilayer domains, *Comput. Methods Appl. Math.* **6** (2006) 306–325.
45. R. Oyarzúa and R. Ruiz-Baier, Locking-free finite element methods for poroelasticity, *SIAM J. Numer. Anal.* **54** (2016) 2951–2973.
46. I. Perugia, P. Pietra and A. Russo, A plane wave virtual element method for the Helmholtz problem, *ESAIM Math. Model. Numer. Anal.* **50** (2016) 783–808.
47. B. Rivière, J. Tan, and T. Thompson, Error analysis of primal discontinuous Galerkin methods for a mixed formulation of the Biot equations, *Comput. Math. Appl.* **73** (2017) 666–683.
48. R.E. Showalter, Diffusion in poro-elastic media, *J. Math. Anal. Appl.* **251** (2000) 310–340.
49. X. Tang, Z. Liu, B. Zhang and M. Feng, On the locking-free three-field virtual element methods for Biot's consolidation model in poroelasticity, *ESAIM: Math. Model. Numer. Anal.* (2020) (Available online: https://doi.org/10.1051/m2an/2020064).
50. G. Vacca, An H^1-conforming virtual element for Darcy and Brinkman equations, *Math. Models Methods Appl. Sci.* **28** (2018) 159–194.
51. G. Vacca and L. Beirão da Veiga, Virtual element methods for parabolic problems on polygonal meshes, *Numer. Methods Partial Differential Equations* **31** (2015) 2110–2134.
52. N. Verma, B. Gómez-Vargas, L.M. De Oliveira Vilaca, S. Kumar, and R. Ruiz-Baier, Well-posedness and discrete analysis for advection-diffusion-reaction in poroelastic media. *Applic. Anal.*, (2020) in press.
53. S.-Y. Yi, A coupling of nonconforming and mixed finite element methods for Biot's consolidation model. *Numer. Methods Partial Differential Equations* **29**(5) (2013) 1749–1777.
54. S.-Y. Yi, A study of two modes of locking in poroelasticity, *SIAM J. Numer. Anal.* **55** (2017) 1915–1936.

Appendix A Proof of Theorem 4.3

As in the semidiscrete case we split the individual errors as

$$\begin{aligned} \boldsymbol{u}(t_n) - \boldsymbol{u}_h^n &= (\boldsymbol{u}(t_n) - I_{\boldsymbol{u}}^h \boldsymbol{u}(t_n)) + (I_{\boldsymbol{u}}^h \boldsymbol{u}(t_n) - \boldsymbol{u}_h^n) := E_{\boldsymbol{u}}^{I,n} + E_{\boldsymbol{u}}^{A,n}, \\ \psi(t_n) - \psi_h^n &= (\psi(t_n) - I_\psi^h \psi(t_n)) + (I_\psi^h \psi(t_n) - \psi_h^n) := E_\psi^{I,n} + E_\psi^{A,n}, \\ p(t_n) - p_h^n &= (p(t_n) - I_p^h p(t_n)) + (I_p^h p(t_n) - p_h^n) := E_p^{I,n} + E_p^{A,n}. \end{aligned}$$

Then, from estimate (4.2a) and following the steps of the proof of Theorem 4.2 we get the bounds

$$\begin{aligned} \|E_{\boldsymbol{u}}^{I,n}\|_1 &\le Ch(|\boldsymbol{u}(t_n)|_2 + |\psi(t_n)|_1) \le Ch(|\boldsymbol{u}(0)|_2 + |\psi(0)|_1 + \|\partial_t \boldsymbol{u}\|_{\boldsymbol{L}^1(0,t_n;[H^2(\Omega)]^2)} \\ &\qquad + \|\partial_t \psi\|_{L^1(0,t_n;H^1(\Omega))}), \end{aligned} \tag{A.1a}$$

$$\|E_\psi^{I,n}\|_0 \le Ch(|\boldsymbol{u}(0)|_2 + |\psi(0)|_1 + \|\partial_t \boldsymbol{u}\|_{\boldsymbol{L}^1(0,t_n;[H^2(\Omega)]^2)} + \|\partial_t \psi\|_{L^1(0,t_n;H^1(\Omega))}), \tag{A.1b}$$

$$\|E_p^{I,n}\|_1 \le Ch(|p(0)|_2 + \|\partial_t p\|_{L^1(0,t_n;H^2(\Omega))}). \tag{A.1c}$$

From equations (4.1a), (3.17a) and (2.3a), we readily get

$$a_1^h(E_{\boldsymbol{u}}^{A,n}, \boldsymbol{v}_h) + b_1(\boldsymbol{v}_h, E_\psi^{A,n}) = F^n(\boldsymbol{v}_h) - F^{h,n}(\boldsymbol{v}_h). \tag{A.2}$$

We then use (4.1b) and (3.21), and proceed to differentiate (2.3c) with respect to time. This implies

$$\begin{aligned} &b_1(E_{\boldsymbol{u}}^{A,n} - E_{\boldsymbol{u}}^{A,n-1}, \phi_h) + b_2(E_p^{A,n} - E_p^{A,n-1}, \phi_h) - a_3(E_\psi^{A,n} - E_\psi^{A,n-1}, \phi_h) \\ &\quad = b_1((\boldsymbol{u}(t_n) - \boldsymbol{u}(t_{n-1})) - (\Delta t)\partial_t \boldsymbol{u}(t_n), \phi_h) + b_2((I_p^h p(t_n) - I_p^h p(t_{n-1})) - (\Delta t)\partial_t p(t_n), \phi_h) \\ &\qquad - a_3((I_\psi^h \psi(t_n) - I_\psi^h \psi(t_{n-1})) - (\Delta t)\partial_t \psi(t_n), \phi_h). \end{aligned} \tag{A.3}$$

After choosing $\boldsymbol{v}_h = E_{\boldsymbol{u}}^{A,n} - E_{\boldsymbol{u}}^{A,n-1}$ in (A.2) and $\phi_h = -E_\psi^{A,n}$ in (A.3) and adding the outcomes, we readily get

$$\begin{aligned} &a_1^h(E_{\boldsymbol{u}}^{A,n}, E_{\boldsymbol{u}}^{A,n} - E_{\boldsymbol{u}}^{A,n-1}) + a_3(E_\psi^{A,n} - E_\psi^{A,n-1}, E_\psi^{A,n}) - b_2(E_p^{A,n} - E_p^{A,n-1}, E_\psi^{A,n}) \\ &\quad = \rho(\boldsymbol{b}(t_n) - \boldsymbol{b}_h^n, E_{\boldsymbol{u}}^{A,n} - E_{\boldsymbol{u}}^{A,n-1})_{0,\Omega} - b_1((\boldsymbol{u}(t_n) - \boldsymbol{u}(t_{n-1})) - (\Delta t)\partial_t \boldsymbol{u}(t_n), E_\psi^{A,n}) \\ &\qquad - b_2((I_p^h p(t_n) - I_p^h p(t_{n-1})) - (\Delta t)\partial_t p(t_n), E_\psi^{A,n}) \\ &\qquad + a_3((I_\psi^h \psi(t_n) - I_\psi^h \psi(t_{n-1})) - (\Delta t)\partial_t \psi(t_n), E_\psi^{A,n}). \end{aligned} \tag{A.4}$$

Next, and as a consequence of using (4.1c), (3.7b) and (2.3b) with $q_h = E_p^{A,n}$, we are left with

$$\begin{aligned} &\tilde{a}_2^h(E_p^{A,n} - E_p^{A,n-1}, E_p^{A,n}) + \Delta t a_2^h(E_p^{A,n}, E_p^{A,n}) - b_2(E_p^{A,n}, E_\psi^{A,n} - E_\psi^{A,n-1}) \\ &\quad = \Delta t(\ell(t_n) - \ell_h^n, E_p^{A,n})_{0,\Omega} + \tilde{a}_2^h(I_p^h p(t_n) - I_p^h p(t_{n-1}), E_p^{A,n}) \\ &\qquad - \tilde{a}_2((\Delta t)\partial_t p(t_n), E_p^{A,n}) + b_2(E_p^{A,n}, (\Delta t)\partial_t \psi - (I_\psi^h \psi(t_n)) - I_\psi^h \psi(t_{n-1})). \end{aligned} \tag{A.5}$$

If we then add the resulting equations (A.4)-(A.5) and repeat the same arguments used in deriving (3.11), we can assert that

$$\begin{aligned} &a_3(E_\psi^{A,n} - E_\psi^{A,n-1}, E_\psi^{A,n}) - b_2(E_p^{A,n} - E_p^{A,n-1}, E_\psi^{A,n}) \\ &\qquad - b_2(E_p^{A,n}, E_\psi^{A,n} - E_\psi^{A,n-1}) + \tilde{a}_2^h(E_p^{A,n} - E_p^{A,n-1}, E_p^{A,n}) \\ &\quad = (\Delta t)\Bigg(c_0(\delta_t E_p^{A,n}, E_p^{A,n})_{0,\Omega} + \frac{1}{\lambda}\sum_K (\alpha^2(\delta_t(I - \Pi_K^0)E_p^{A,n}, (I - \Pi_K^0)E_p^{A,n})_{0,K} \\ &\qquad - (\delta_t(\alpha \Pi_K^0 E_p^{A,n} - E_\psi^{A,n}), \alpha \Pi_K^0 E_p^{A,n} - E_\psi^{A,n})_{0,K})\Bigg), \end{aligned}$$

The left-hand side can be bounded by using the inequality (3.24) and then summing over n we get

$$\begin{aligned} &\mu\|\boldsymbol{\varepsilon}(E_{\boldsymbol{u}}^{A,n})\|_0^2 + c_0\|E_p^{A,n}\|_0^2 + (\Delta t)\frac{\kappa_{\min}}{\eta}\sum_{j=1}^n \|\nabla E_p^{A,j}\|_0^2 \\ &\quad + (1/\lambda)\sum_K \left(\alpha^2\|(I - \Pi_K^0)E_p^{A,n}\|_{0,K}^2 + \|\alpha \Pi_K^0 E_p^{A,n} - E_\psi^{A,n}\|_{0,K}^2\right) \\ &\le \mu\|\boldsymbol{\varepsilon}(E_{\boldsymbol{u}}^{A,0})\|_0^2 + c_0\|E_p^{A,0}\|_0^2 + (1/\lambda)\sum_K \left(\alpha^2\|(I - \Pi_K^0)E_p^{A,0}\|_{0,K}^2 + \|\alpha \Pi_K^0 E_p^{A,0} - E_\psi^{A,0}\|_{0,K}^2\right) \end{aligned}$$

$$
\begin{aligned}
&+\underbrace{\sum_{j=1}^{n}\rho(\boldsymbol{b}(t_j)-\boldsymbol{b}_h^j,E_{\boldsymbol{u}}^{A,j}-E_{\boldsymbol{u}}^{A,j-1})_{0,\Omega}}_{=:L_1}+\underbrace{\sum_{j=1}^{n}\Delta t(\ell(t_j)-\ell_h^j,E_p^{A,j})_{0,\Omega}}_{=:L_2}\\
&-\underbrace{\sum_{j=1}^{n}b_1((\boldsymbol{u}(t_j)-\boldsymbol{u}(t_{j-1}))-(\Delta t)\partial_t\boldsymbol{u}(t_j),E_\psi^{A,j})}_{=:L_3}\\
&-\underbrace{\sum_{j=1}^{n}b_2((I_p^hp(t_j)-I_p^hp(t_{j-1}))-(\Delta t)\partial_tp(t_j),E_\psi^{A,j})}_{=:L_4}\\
&+\underbrace{\sum_{j=1}^{n}a_3((I_\psi^h\psi(t_j)-I_\psi^h\psi(t_{j-1}))-(\Delta t)\partial_t\psi(t_j),E_\psi^{A,j})}_{:=L_5}\\
&+\underbrace{\sum_{j=1}^{n}(\tilde a_2^h(I_p^hp(t_j)-I_p^hp(t_{j-1}),E_p^{A,j})-\tilde a_2((\Delta t)\partial_tp(t_j),E_p^{A,j}))}_{:=L_6}\\
&+\underbrace{\sum_{j=1}^{n}b_2(E_p^{A,j},(\Delta t)\partial_t\psi-(I_\psi^h\psi(t_j)-I_\psi^h\psi(t_{j-1}))}_{:=L_7}.
\end{aligned}
$$

We bound the term L_1 with the help of formula (3.25), the estimates of projection $\boldsymbol{\Pi}_K^{0,0}$, applying Taylor expansion, and using the generalised Young's inequality. This gives

$$
\begin{aligned}
L_1&=\rho\big(((\boldsymbol{b}-\boldsymbol{b}_h)(t_n),E_{\boldsymbol{u}}^{A,n})_{0,\Omega}-((\boldsymbol{b}-\boldsymbol{b}_h)(0),E_{\boldsymbol{u}}^{A,0})_{0,\Omega}-\sum_{j=1}^{n}(\Delta t)(\delta_t(\boldsymbol{b}-\boldsymbol{b}_h)(t_j),E_{\boldsymbol{u}}^{A,j-1})_{0,\Omega})\big)\\
&\le\frac{\mu}{2}\|\boldsymbol{\varepsilon}(E_{\boldsymbol{u}}^{A,n})\|_0^2+C_1\Big(\frac{\rho}{\mu}h|b(0)|_1\;\mu\|\boldsymbol{\varepsilon}(E_{\boldsymbol{u}}^{A,0})\|_0+\frac{\rho^2}{\mu}h^2\max_{1\le j\le n}|\boldsymbol{b}(t_j)|_1^2\\
&\qquad+(\Delta t)\;h\sum_{j=1}^{n}\frac{\rho}{\mu}\Big(|\partial_t\boldsymbol{b}^j|_1+\big(\Delta t\int_{t_{j-1}}^{t_j}|\partial_{tt}\boldsymbol{b}(s)|_1^2\,\mathrm{d}s\big)^{1/2}\Big)\mu\|\boldsymbol{\varepsilon}(E_{\boldsymbol{u}}^{A,j-1})\|_0\Big).
\end{aligned}
$$

Then the estimate satisfied by the projection Π_K^0 along with Poincaré and Young's inequalities, yield

$$
L_2\le C_2\sum_{j=1}^{n}(\Delta t)h|\ell(t_j)|_1\|\nabla E_p^{A,j}\|_0\le C_2\sum_{j=1}^{n}(\Delta t)\frac{\eta}{\kappa_{\min}}h^2|\ell(t_j)|_1^2+(\Delta t)\frac{\kappa_{\min}}{6\eta}\sum_{j=1}^{n}\|\nabla E_p^{A,j}\|_0^2.
$$

The discrete inf-sup condition (3.6) implies that

$$
\|E_\psi^{A,j}\|_0\le C(h|\boldsymbol{b}(t_j)|_1+\|\boldsymbol{\varepsilon}(E_{\boldsymbol{u}}^{A,j})\|_0). \tag{A.6}
$$

Applying an expansion in Taylor series, together with (A.6), the Cauchy-Schwarz, and Young inequalities, enable us to write

$$
L_3\le C\sum_{j=1}^{n}\Big((\Delta t)^3\int_{t_{j-1}}^{t_j}\|\partial_{tt}\boldsymbol{u}(s)\|_0^2\,\mathrm{d}s\Big)^{1/2}(h|\boldsymbol{b}(t_j)|_1+\|\boldsymbol{\varepsilon}(E_{\boldsymbol{u}}^{A,j})\|_0).
$$

Then, after using the estimates of the projection I_p^h (4.2b), (A.6), and applying again Cauchy-Schwarz inequality, we get

$$
\begin{aligned}
L_4&\le C\frac{\alpha}{\lambda}\sum_{j=1}^{n}\Big(\|I_p^h(p(t_j)-p(t_{j-1}))-(p(t_j)-p(t_{j-1}))\|_0+\|(p(t_j)-p(t_{j-1}))-(\Delta t)\partial_tp(t_j)\|_0\Big)\|E_\psi^{A,j}\|_0\\
&\le C\frac{\alpha}{\lambda}\sum_{j=1}^{n}\Big(h^2\Big((\Delta t)\int_{t_{j-1}}^{t_j}|\partial_tp(s)|_2^2\,\mathrm{d}s\Big)^{1/2}+\Big((\Delta t)^3\int_{t_{j-1}}^{t_j}\|\partial_{tt}p(s)\|_0^2\,\mathrm{d}s\Big)^{1/2}\Big)\|E_\psi^{A,j}\|_0\\
&\le C\frac{\alpha}{\lambda}\sum_{j=1}^{n}\Big(h^2\Big((\Delta t)\int_{t_{j-1}}^{t_j}|\partial_tp(s)|_2^2\,\mathrm{d}s\Big)^{1/2}+\Big((\Delta t)^3\int_{t_{j-1}}^{t_j}\|\partial_{tt}p(s)\|_0^2\,\mathrm{d}s\Big)^{1/2}\Big)(\rho h|\boldsymbol{b}(t_j)|_1+\|\boldsymbol{\varepsilon}(E_{\boldsymbol{u}}^{A,j})\|_0).
\end{aligned}
$$

The stability of $a_3(\cdot,\cdot)$ and the proof for the bound of L_4 gives

$$
\begin{aligned}
L_5 &\leq C(1/\lambda)\sum_{j=1}^{n}\|(I_\psi^h\psi(t_j)-I_\psi^h\psi(t_{j-1}))-(\Delta t)\partial_t\psi(t_j)\|_0(\rho h|\boldsymbol{b}(t_j)|_1+\|\boldsymbol{\varepsilon}(E_{\boldsymbol{u}}^{A,j})\|_0)\\
&\leq C(1/\lambda)\sum_{j=1}^{n}\Big(h^2\Big((\Delta t)\int_{t_{j-1}}^{t_j}(|\partial_t\boldsymbol{u}(s)|_2^2+|\partial_t\psi(s)|_1^2)\,\mathrm{d}s\Big)^{1/2}+\Big((\Delta t)^3\int_{t_{j-1}}^{t_j}\|\partial_{tt}\psi(s)\|_0^2\,\mathrm{d}s\Big)^{1/2}\Big)\\
&\qquad\times(\rho h|\boldsymbol{b}(t_j)|_1+\|\boldsymbol{\varepsilon}(E_{\boldsymbol{u}}^{A,j})\|_0).
\end{aligned}
$$

The polynomial approximation p_π for fluid pressure, consistency of the bilinear form $\tilde{a}_2^h(\cdot,\cdot)$, stability of the bilinear forms $\tilde{a}_2(\cdot,\cdot),\tilde{a}_2^h(\cdot,\cdot)$, the Cauchy-Schwarz, Poincaré and Young's inequalities gives

$$
\begin{aligned}
L_6 &= \sum_{j=1}^{n}\Big(\tilde{a}_2^h((I_p^hp(t_j)-I_p^hp(t_{j-1}))-(p_\pi(t_j)-p_\pi(t_{j-1})),E_p^{A,j})\\
&\qquad+\tilde{a}_2((p_\pi(t_j)-p_\pi(t_{j-1}))-(p(t_j)-p(t_{j-1})),E_p^{A,j})+\tilde{a}_2((p(t_j)-p(t_{j-1}))-(\Delta t)\partial_tp(t_j),E_p^{A,j})\Big)\\
&\leq C\Big(c_0+\frac{\alpha^2}{\lambda}\Big)\sum_{j=1}^{n}\Big(h^2\Big((\Delta t)\int_{t_{j-1}}^{t_j}|\partial_tp(s)|_2^2\,\mathrm{d}s\Big)^{1/2}+\Big((\Delta t)^3\int_{t_{j-1}}^{t_j}\|\partial_{tt}p(s)\|_0^2\,\mathrm{d}s\Big)^{1/2}\Big)\|\nabla E_p^{A,j}\|_0\\
&\leq C\Big(c_0+\frac{\alpha^2}{\lambda}\Big)^2\Big(h^4\|\partial_tp\|^2_{L^2(0,t_n;H^2(\Omega))}+(\Delta t)^2\|\partial_{tt}p\|^2_{L^2(0,t_n;L^2(\Omega))}\Big)+\Delta t\frac{\kappa_{\min}}{6\eta}\sum_{j=1}^{n}\|\nabla E_p^{A,j}\|_0^2.
\end{aligned}
$$

The continuity of $b_2(\cdot,\cdot)$, the bound derived for the term L_5 and using the Young's inequality gives

$$
\begin{aligned}
L_7 &\leq \frac{\alpha}{\lambda}\sum_{j=1}^{n}\|(\Delta t)\partial_t\psi(t_j)-(I_\psi^h\psi(t_j)-I_\psi^h\psi(t_{j-1}))\|_0\|E_p^{A,j}\|_0\\
&\leq C\Big(\frac{\alpha}{\lambda}\Big)^2\Big(h^2(\|\partial_t\psi\|^2_{L^2(0,t_n;H^1(\Omega))}+\|\partial_t\boldsymbol{u}\|^2_{\boldsymbol{L}^2(0,t_n;[H^2(\Omega)]^2)})+(\Delta t)^2\|\partial_{tt}\psi\|^2_{L^2(0,t_n;L^2(\Omega))}\Big)\\
&\qquad+(\Delta t)\frac{\kappa_{\min}}{6\eta}\sum_{j=1}^{n}\|\nabla E_p^{A,j}\|_0^2.
\end{aligned}
$$

In turn, putting together the bounds obtained for all L_i's, $i=1,\ldots,7$, using the Young's inequality and Lemma 3.2 concludes that

$$
\begin{aligned}
&\mu\|\boldsymbol{\varepsilon}(E_{\boldsymbol{u}}^{A,n})\|_0^2+c_0\|E_p^{A,n}\|_0^2+(\Delta t)\frac{\kappa_{\min}}{\eta}\sum_{j=1}^{n}\|\nabla E_p^{A,j}\|_0^2\\
&\leq C\Big(\mu\|\boldsymbol{\varepsilon}(E_{\boldsymbol{u}}^{A,0})\|_0^2+(c_0+\alpha^2/\lambda)\|E_p^{A,0}\|_0^2+(1/\lambda)\|E_\psi^{A,0}\|_0^2+\Big(1+\Delta t\Big)h^2\max_{0\leq j\leq n}|\boldsymbol{b}(t_j)|_1^2\\
&\quad+h^2\Delta t\sum_{j=1}^{n}(|\boldsymbol{b}(t_j)|_1^2+(\Delta t)|\partial_t\boldsymbol{b}|_1^2+|\ell(t_j)|_1^2)+(\Delta t)^2h^2\|\partial_{tt}\boldsymbol{b}\|_{L^2(0,t_n;[H^1(\Omega)]^2)}\\
&\quad+(\Delta t)^2\big((c_0+\alpha^2/\lambda)^2\|\partial_{tt}p\|^2_{L^2(0,t_n;L^2(\Omega))}+\|\partial_{tt}\boldsymbol{u}\|^2_{\boldsymbol{L}^2(0,t_n;[L^2(\Omega)]^2)}+\frac{\alpha^2}{\lambda^2}\|\partial_{tt}\psi\|^2_{L^2(0,t_n;L^2(\Omega))}\big)\\
&\quad+h^2\big(\frac{\alpha^2}{\lambda^2}\|\partial_t\psi\|^2_{L^2(0,t_n;H^1(\Omega))}+\frac{\alpha^2}{\lambda^2}\|\partial_t\boldsymbol{u}\|^2_{\boldsymbol{L}^2(0,t_n;[H^2(\Omega)]^2)}+(c_0+\alpha^2/\lambda)^2h^2\|\partial_tp\|^2_{L^2(0,t_n;H^2(\Omega))}\big)\Big).
\end{aligned}
$$

And finally, the desired result (4.9) holds after choosing $\boldsymbol{u}_h^0:=\boldsymbol{u}_I(0)$, $\psi_h^0:=\Pi^{0,0}\psi(0)$, $p_h^0:=p_I(0)$ and applying triangle's inequality together with (A.1a)-(A.1c) and (A.6).